RESEARCH ARTICLE

AMERICAN JOURNAL OF medical genetics PART A

# *MLL2* and *KDM6A* Mutations in Patients With Kabuki Syndrome

**Noriko Miyake,[1]* Eriko Koshimizu,[1] Nobuhiko Okamoto,[2] Seiji Mizuno,[3] Tsutomu Ogata,[4] Toshiro Nagai,[5] Tomoki Kosho,[6] Hirofumi Ohashi,[7] Mitsuhiro Kato,[8] Goro Sasaki,[9] Hiroyo Mabe,[10] Yoriko Watanabe,[11] Makoto Yoshino,[11] Toyojiro Matsuishi,[11] Jun-ichi Takanashi,[12] Vorasuk Shotelersuk,[13] Mustafa Tekin,[14] Nobuhiko Ochi,[15] Masaya Kubota,[16] Naoko Ito,[17] Kenji Ihara,[17] Toshiro Hara,[17] Hidefumi Tonoki,[18] Tohru Ohta,[19] Kayoko Saito,[20] Mari Matsuo,[20] Mari Urano,[20] Takashi Enokizono,[21] Astushi Sato,[22] Hiroyuki Tanaka,[23] Atsushi Ogawa,[24] Takako Fujita,[25] Yoko Hiraki,[26] Sachiko Kitanaka,[22] Yoichi Matsubara,[27] Toshio Makita,[28] Masataka Taguri,[29] Mitsuko Nakashima,[1] Yoshinori Tsurusaki,[1] Hirotomo Saitsu,[1] Ko-ichiro Yoshiura,[30] Naomichi Matsumoto,[1]* and Norio Niikawa[19]**

[1]Department of Human Genetics, Yokohama City University Graduate School of Medicine, Yokohama, Japan

[2]Department of Medical Genetics, Osaka Medical Center and Research Institute for Maternal and Child Health, Izumi, Japan

[3]Department of Pediatrics, Central Hospital, Aichi Human Service Center, Kasugai, Japan

[4]Department of Pediatrics, Hamamatsu University School of Medicine, Hamamatsu, Japan

[5]Department of Pediatrics, Dokkyo Medical University Koshigaya Hospital, Saitama, Japan

[6]Department of Medical Genetics, Shinshu University School of Medicine, Matsumoto, Japan

[7]Division of Medical Genetics, Saitama Children's Medical Center, Iwatsuki, Japan

[8]Department of Pediatrics, Yamagata University Faculty of Medicine, Yamagata, Japan

[9]Department of Pediatrics, Tokyo Dental College Ichikawa General Hospital, Chiba, Japan

[10]Department of Child Development, Kumamoto University Hospital, Kumamoto, Japan

[11]Department of Pediatrics and Child Health, Kurume University School of Medicine, Kurume, Japan

[12]Department of Pediatrics, Kameda Medical Center, Kamogawa, Chiba, Japan

[13]Center of Excellence for Medical Genetics, Department of Pediatrics, Faculty of Medicine, Chulalongkorn University, Bangkok, Thailand

[14]John P. Hussman Institute for Human Genomics, Miller School of Medicine, University of Miami, Miami, Florida

[15]Department of Pediatrics, Aichi Prefectural Hospital and Habilitation Center for Disabled Children, Dai-ni Aoitori Gakuen, Okazaki, Japan

[16]Division of Neurology, National Center for Child Health and Development, Tokyo, Japan

[17]Department of Pediatrics, Graduate School of Medical Sciences, Kyushu University, Fukuoka, Japan

[18]Section of Clinical Genetics, Department of Pediatrics, Tenshi Hospital, Sapporo, Japan

[19]Research Institute of Personalized Health Sciences, Health Science University of Hokkaido, Tobetsu, Japan

[20]Institute of Medical Genetics, Tokyo Women's Medical University, Tokyo, Japan

[21]Department of Pediatrics, University of Tsukuba Hospital, Tsukuba, Japan

[22]Department of Pediatrics, Graduate School of Medicine, The University of Tokyo, Tokyo, Japan

[23]Department of Pediatrics, Ohta Nishinouchi Hospital, Tokyo, Japan

[24]Department of Pediatrics, Chikushi Hospital, Fukuoka University, Fukuoka, Japan

[25]Department of Pediatrics, Fukuoka University School of Medicine, Fukuoka, Japan

[26]Hiroshima Municipal Center for Child Health and Development, Hiroshima, Japan

[27]Department of Medical Genetics, Tohoku University School of Medicine, Sendai, Japan

[28]Education Center, Asahikawa Medical University, Asahikawa, Japan

[29]Department of Biostatistics and Epidemiology, Yokohama City University Graduate School of Medicine, Yokohama, Japan

[30]Department of Human Genetics, Graduate School of Biomedical Sciences, Nagasaki University, Nagasaki, Japan

Manuscript Received: 9 January 2013; Manuscript Accepted: 9 May 2013

Kabuki syndrome is a congenital anomaly syndrome characterized by developmental delay, intellectual disability, specific facial features including long palpebral fissures and ectropion of the lateral third of the lower eyelids, prominent digit pads, and skeletal and visceral abnormalities. Mutations in *MLL2* and *KDM6A* cause Kabuki syndrome. We screened 81 individuals with Kabuki syndrome for mutations in these genes by conventional methods (n = 58) and/or targeted resequencing (n = 45) or whole exome sequencing (n = 5). We identified a mutation in *MLL2* or *KDM6A* in 50 (61.7%) and 5 (6.2%) cases, respectively. Thirty-five *MLL2* mutations and two *KDM6A* mutations were novel. Non-protein truncating-type *MLL2* mutations were mainly located around functional domains, while truncating-type mutations were scattered through the entire coding region. The facial features of patients in the *MLL2* truncating-type mutation group were typical based on those of the 10 originally reported patients with Kabuki syndrome; those of the other groups were less typical. High arched eyebrows, short fifth finger, and hypotonia in infancy were more frequent in the *MLL2* mutation group than in the *KDM6A* mutation group. Short stature and postnatal growth retardation were observed in all individuals with *KDM6A* mutations, but in only half of the group with *MLL2* mutations. © 2013 Wiley Periodicals, Inc.

**Key words:** Kabuki syndrome; *MLL2*; *KDM6A*; mutation; genotype–phenotype correlation

**How to Cite this Article:**
Miyake N, Koshimizu E, Okamoto N, Mizuno S, Ogata T, Nagai T, Kosho T, Ohashi H, Kato M, Sasaki G, Mabe H, Watanabe Y, Yoshino M, Matsuishi T, Takanashi J-i, Shotelersuk V, Tekin M, Ochi N, Kubota M, Ito N, Ihara K, Hara T, Tonoki H, Ohta T, Saito K, Matsuo M, Urano M, Enokizono T, Sato A, Tanaka H, Ogawa A, Fujita T, Hiraki Y, Kitanaka S, Matsubara Y, Makita T, Taguri M, Nakashima M, Tsurusaki Y, Saitsu H, Yoshiura K-i, Matsumoto N, Niikawa N. 2013. *MLL2* and *KDM6A* mutations in patients with Kabuki syndrome.
Am J Med Genet Part A 161A:2234–2243.

## INTRODUCTION

Kabuki syndrome (KS; OMIM 147920) is a multiple congenital anomaly syndrome that was originally reported by Niikawa et al. [1981] and Kuroki et al. [1981] (also known as Kabuki make-up syndrome or Niikawa–Kuroki syndrome). KS is diagnosed clinically by characteristic facial features, including long palpebral fissures and ectropion of the lateral third of the lower eyelids, postnatal growth impairment (short stature), developmental delay, intellectual disability, dermatoglyphic abnormalities, visceral and skeletal abnormalities, and immunological dysfunction. The prevalence of the disorder is estimated to be 1 in 32,000 live births [Niikawa et al., 1988]. Two genes have shown to be mutated in patients with KS: *MLL2* (myeloid/lymphoid or mixed-lineage leukemia 2; NM_003482.3) at 12q13.12 and *KDM6A* (lysine (K)-specific demethylase 6A; NM_021140.2) at Xp11.3 [Ng et al., 2010; Lederer et al., 2012; Miyake et al., 2013]. *MLL2* encodes a histone H3 lysine 4 (H3K4)-specific methyl transferase and KDM6A is a specific demethylase of histone H3 lysine 27 (H3K27) [Prasad et al., 1997; Lee et al., 2007]. They are both trithorax group proteins and bind each other [Schuettengruber et al., 2007]. These proteins are important for the chromatin state and transcription activation: MLL2 methylates H3K4 and KMD6A removes the H3K27 trimethylation repressive mark [Dubuc et al., 2013]. The loss of MLL2 or KDM6A function may lead to repressed transcription [Dubuc et al., 2013].

To our knowledge, there has been no comprehensive screen for mutations in these two genes in the same patient series. In this report, we performed a mutation screen of both genes in 81 patients with KS. We then evaluated the clinical features based on the genetic information.

## MATERIALS AND METHODS

### Samples

Eighty-one individuals clinically suspected to have KS were incorporated in this study: 77 Japanese, two Caucasians, one Belgian, and one Thai. They were all sporadic except for KMS-79, who had an affected sibling. Peripheral blood samples or saliva samples from the

Additional supporting information may be found in the online version of this article at the publisher's web-site.

Conflict of interest: none.
Grant sponsor: Ministry of Health, Labour and Welfare of Japan; Grant sponsor: Japan Science and Technology Agency; Grant sponsor: Strategic Research Program for Brain Sciences; Grant sponsor: Ministry of Education, Culture, Sports, Science and Technology of Japan; Grant sponsor: Grant-in-Aid for Scientific Research from the Japan Society for the Promotion of Science; Grant sponsor: Grant-in-Aid for Young Scientists from the Japan Society for the Promotion of Science; Grant sponsor: Takeda Science Foundation; Grant sponsor: Yokohama Foundation for the Advancement of Medical Science; Grant sponsor: Hayashi Memorial Foundation for Female Natural Scientists.

*Correspondence to:
Dr. Noriko Miyake or Prof. Naomichi Matsumoto, Department of Human Genetics, Yokohama City University Graduate School of Medicine, 3-9 Fukuura, Kanazawa-ku, Yokohama 236-0004, Japan.
E-mails: nmiyake@yokohama-cu.ac.jp (N. Miyake) or naomat@yokohama-cu.ac.jp (N. Matsumoto)

Article first published online in Wiley Online Library (wileyonlinelibrary.com): 2 August 2013
DOI 10.1002/ajmg.a.36072

patients and their parents (when available) were collected with informed consent and DNA was extracted using a QuickGene-610L (Fujifilm, Tokyo, Japan) or Oragene-DNA kit (DNA Genotek, Inc., Ottawa, Canada) according to the manufacturer's instructions. This study included four previously reported patients (KMS-50, KMS-51, KMS-61, and KMS-71) [Tekin et al., 2006; Torii et al., 2009; Ito et al., 2012]. In addition, three patients with a *KDM6A* mutation were previously described as Patients 1, 2, and 3 by Miyake et al. [2013], and are named KMS-31, KMS-37, and KMS-65, respectively, in this report. This study was approved by the Institutional Review Board of Yokohama City University School of Medicine.

## Mutation Screening

Fifty-eight patients (KMS-01 to KMS-69) were screened for *MLL2* mutations by the high-resolution melting (HRM) method using a LightCycler 480 System II (Roche Diagnostics, Indianapolis, IN) and subsequent Sanger sequencing. If an HRM curve pattern was different from those of controls, the DNA sample was Sanger sequenced on an ABI 3500xl or 3130xl Genetic Analyzer (Applied Biosystems, Foster City, CA) and the sequences were analyzed using Sequencher software version 4.10.1 (Gene Codes Corporation, Ann Arbor, MI). *KDM6A* was analyzed in samples with no *MLL2* mutation using HRM analysis and Sanger sequencing as above (n = 37). For male samples, genotyping using spike-in control male genomic DNA (10%) was performed to detect a hemizygous mutation. The latter 23 patients (KMS-70 to KMS-92), as well as 22 patients with no mutation in either gene detected by conventional methods, were analyzed by targeted resequencing as described in the following section. We judged a variant as pathogenic when it was previously reported to cause KS, or novel variant when it was not observed in unaffected parents or in in-house exome data (n = 977), dbSNP135, or EVS6500 (Exome Variant Server, NHLBI GO Exome Sequencing Project, Seattle, WA; http://evs.gs.washington.edu/EVS/; accessed March 1, 2013). In addition, the missense mutation predicted to be polymorphism by both of two predictions (Polyphen-2: http://genetics.bwh.harvard.edu/pph2/ [Adzhubei et al., 2010] and MutationTaster: http://www.mutationtaster.org/ [Schwarz et al., 2010]) was considered to be non-pathogenic. Parentage analysis was conducted for the patients only when the parental samples were available. TaKaRa Ex Taq and TaKaRa LA Taq (both Takara, Tokyo, Japan) were used for amplification. The primer sequences and PCR conditions are available on request. All pathological variants were confirmed by Sanger sequencing. Nucleotide numbering reflects cDNA numbering with +1 corresponding to the A of the ATG translation initiation codon in the reference sequence (RefSeq NM_003482.3 for *MLL2*, RefSeq NM_021140.2 for *KDM6A*).

## Targeted Resequencing of *MLL2* and *KDM6A* by Next-Generation Sequencing

Ion AmpliSeq Custom Panels (Life Technologies, Inc., Grand Island, NY) covering the entire coding region of *MLL2* and *KDM6A* were created via the Ion AmpliSeq Designer v1.2 (https://ampliseq.com/browse.action). Libraries were prepared using the Ion AmpliSeq Library Kit 2.0 (Life Technologies, Inc.), with 10 ng of genomic DNA for each primer pool (two pools for this analysis). An Agilent 2200 TapeStation (Agilent Technologies, Santa Clara, CA) and the associated High Sensitivity D1K Screen Tape (Agilent Technologies) were used to check the size distribution and the concentration of the DNA libraries. Emulsion PCR and enrichment steps were carried out using the Ion OneTouch 200 Template Kit v2 (Life Technologies, Inc.). The amplicon libraries were sequenced on an Ion Torrent Personal Genome Machine system using 314 or 316 chips, and bar-coding was applied with an Ion Xpress Barcode Adapters 1–16 Kit (all Life Technologies, Inc.). Torrent Suite 2.2 (Life Technologies, Inc.) was used for mapping, base calling, and variant calling. Sequences were annotated using SeattleSeq Annotation 134 (http://snp.gs.washington.edu/SeattleSeqAnnotation134/). All variants were confirmed by Sanger sequencing.

## Whole Exome Sequencing by High-Throughput Next-Generation Sequencing

Whole exome sequencing was performed in five individuals (KMS-09, -18, -21, -23, and -61) who had no *MLL2* or *KDM6A* abnormality by HRM analysis. DNA was processed with a SureSelect Human All Exon V4 kit (Agilent Technologies), sequenced on a HiSeq2000 (Illumina, Inc., San Diego, CA), and analyzed as previously described [Tsurusaki et al., 2013]. Variants in *MLL2* and *KDM6A* were confirmed by Sanger sequencing.

## X-Inactivation Assay

X-inactivation analysis was performed as described [Allen et al., 1992] with slight modification. Briefly, genomic DNA (500 ng) was digested with two methylation-sensitive restriction enzymes, *Hpa*II and *Hha*I (New England Biolabs, Beverly, MA), and purified by phenol/chloroform extraction and ethanol precipitation. Digested and undigested DNA samples (10 ng) were separately amplified for the (CAG)*n* polymorphism at the androgen receptor locus. The forward primer was labeled with 5′ FAM dye. PCR products were analyzed on an ABI 3500xl Genetic Analyzer using GeneMapper Software Version 4.1 (Applied Biosystems). The assay was independently performed twice.

## cDNA Sequencing

Total RNA was extracted from a lymphoblastoid cell line established from KMS-81 (c.1909_1912del in *KDM6A*) using an RNeasy Plus mini kit (Qiagen, Hilden, Germany) with and without cycloheximide treatment (30 μg/ml) for 4 hr before cell collection. Reverse transcription (RT) was performed using a Superscript III First-Strand synthesis system for RT-PCR (Life Technologies, Inc.). As the mutation was located in exon 17, the region from the exon 15/16 boundary to the exon 17/18 boundary of *KDM6A* was amplified using cDNA-specific primer pairs (sequences available on request) and sequenced by the Sanger method.

## Statistical Analysis

The frequencies of clinical features in the two groups were compared by Fisher's exact test. A difference was considered statistically

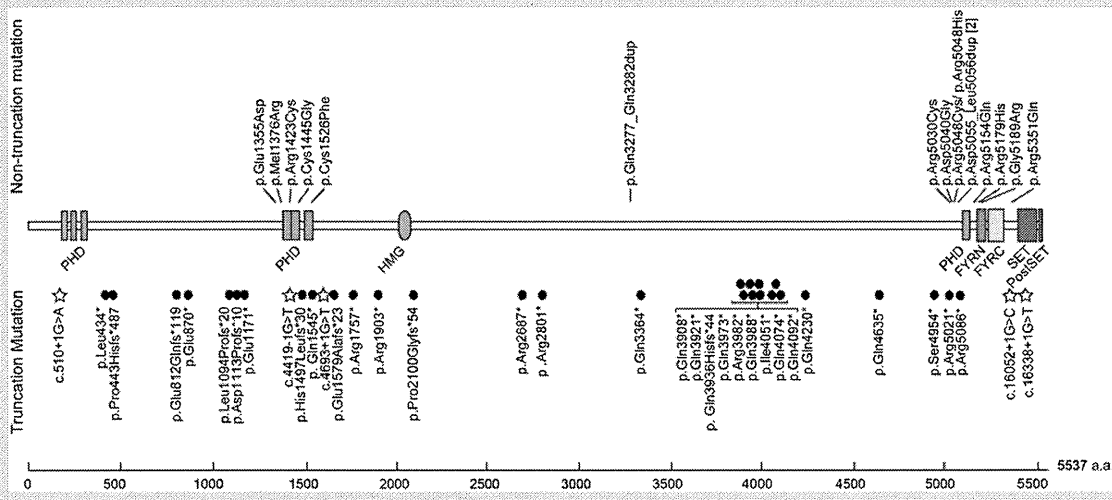


**FIG. 1.** ***MLL2*** **mutations in patients with Kabuki syndrome. Upper: Non-truncating-type mutations. Middle: MLL2 protein structure with functional domains. The protein contains seven plant homeodomains (PHD), one high-mobility group (HMG) domain, a Phe-Tyr-rich *N*-terminal (FYRN) domain, a Phe-Tyr-rich *C*-terminal (FYRC) domain, a SET (Suvar3-9, Enhancer-of-zeste, Trithorax) domain, and a PostSET domain. These functional domains were based on a prediction by SMART (http://smart.embl-heidelberg.de/) and the UniProtKB database (http://www.uniprot.org/uniprot/O14686). Lower: Truncating-type mutations. Black circles denote nonsense mutations or frameshift mutations. Stars represent splice-site mutations.**

significant if $P < 0.05$. Correction for multiple testing was not applied.

## RESULTS

### Overall Mutation Detection Rates

Pathogenic mutations in *MLL2* and *KDM6A* were found in 50 (61.7%) and five (6.2%) of the 81 patients with KS, respectively (Figs. 1 and 2, Tables I and II). Of the 50 *MLL2* mutations, 35 (70.0%) were predicted to be protein truncating-type and 15 (30.0%) were predicted to be non-truncating-type. Interestingly, non-truncating mutations were mostly localized in or adjacent to the functional domains, while truncating mutations were scattered throughout the entire coding region (Fig. 1). Fifteen of the *MLL2* mutations have been previously reported (Table I). Three novel variants (not included in the 50 mutations) were considered non-pathogenic (Supplemental Table I). Variant c.10942C > G in patient KMS-22 was predicted to be benign by Polyphen-2 and MutationTaster, c.8813C > T in patient KMS-62 was inherited from an unaffected father, and c.4065A > T in KMS-75 was found heterozygously in our 977 in-house controls. An in-frame duplication in patients KMS-40 and KMS-62, which predicted p.Asp5055_Leu5056dup, was predicted to be polymorphic by MutationTaster, but was previously reported as a pathogenic mutation [Micale et al., 2011]. In addition, the other in-frame mutation in KMS-02 was also predicted to be polymorphic. Unfortunately, parental samples were unavailable for these individuals, except for the mother of patient KMS-62, who did not have this mutation; thus, the de novo status remains unclear. Of the five *KDM6A* mutations including three mutations reported previously [Miyake et al., 2013], four were truncating-type and one was an in-frame deletion located within the Jumonji C domain (Fig. 2).

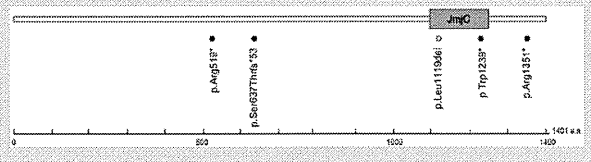


**FIG. 2.** ***KDM6A*** **mutations in patients with Kabuki syndrome. Upper: Scheme of KDM6A protein. It contains a Jumonji C (JmjC) domain (purple box). Lower: Black circles indicate truncating-type mutations (nonsense or frameshift mutations); the white circle represents a non-truncating-type mutation (in-frame deletion).**

### Clinical Comparison Between the Mutation-Positive and -Negative Groups

We compared the clinical features of the *MLL2* or *KDM6A* mutation-positive and -negative groups (Supplemental Table II). Long palpebral fissures were observed in almost all patients. Cleft lip/palate was more frequently observed in the mutation-positive group ($P = 0.0197$). Interestingly, developmental delay and intellectual disability were observed in all individuals with mutations but were unobserved in some mutation-negative cases ($P = 0.0314$

TABLE I. *MLL2* and *KDM6A* Mutations in Patients With KS

| Patient ID | Method | Mutation | Predicted amino acid change | De novo | Remarks[a] |
|---|---|---|---|---|---|
| Patients with *MLL2* mutations | | | | | |
| KMS-02 | H | c.9831_9848dup | p.Gln3277_Gln3282dup | Unknown | Novel |
| KMS-08 | H | c.12688C > T | p.Gln4230* | Yes | Hannibal et al. [2011] |
| KMS-13 | H | c.2433_2434insCA | p.Glu812Glnfs*119 | Yes | Novel |
| KMS-14 | H | c.11806_11807dup | p. Gln3936Hisfs*44 | Yes | Novel |
| KMS-15 | H | c.15119A > G | p.Asp5040Gly | Yes | Novel |
| KMS-17 | H | c.5707C > T | p.Arg1903* | Yes | Novel |
| KMS-18 | W | c.12151delA | p.Ile4051* | Yes | Novel |
| KMS-20 | H | c.1300delC | p.Leu434* | Unknown | Novel |
| KMS-21 | W | c.3326_3336dup | p.Asp1113Profs*10 | Unknown | Novel |
| KMS-22 | H | c.4127T > G | p.Met1376Arg | Unknown | Novel |
| KMS-23 | W | c.15461G > A | p.Arg5154Gln | Unknown | Li et al. [2011] |
| KMS-24 | H | c.2608 G > T | p.Glu870* | Unknown | Novel |
| KMS-25 | H | c.11917C > T | p.Gln3973* | Unknown | Novel |
| KMS-27 | H | c.15142C > T | p.Arg5048Cys | Yes | Hannibal et al. [2011], Makrythanasis et al. [2013] |
| KMS-28 | H | c.14861C > A | p.Ser4954* | Unknown | Novel |
| KMS-29 | H | c.4419-1G > T | splice site | Unknown | Novel |
| KMS-30 | H | c.4633C > T | p. Gln1545* | Unknown | Novel |
| KMS-32 | H | c.8059C > T | p.Arg2687* | Unknown | Banka et al. [2012b] |
| KMS-33 | T | c.11962C > T | p.Gln3988* | Unknown | Novel |
| KMS-36 | H | c.4736_4737delAG | p.Glu1579Alafs*23 | Unknown | Novel |
| KMS-38 | H | c.15143G > A | p.Arg5048His | Unknown | Makrythanasis et al. [2013] |
| KMS-40 | T | c.15163_15168dup | p.Asp5055_Leu5056dup | Unknown | Micale et al. [2011] |
| KMS-41 | H | c.1328delC | p.Pro443Hisfs*487 | Yes | Ng et al. [2010] |
| KMS-42 | H | c.16052G > A | p.Arg5351Gln | Yes | Novel |
| KMS-43 | H | c.510 + 1G > A | splice site | Unknown | Novel |
| KMS-49 | T | c.15565G > A | p.Gly5189Arg | Unknown | Novel |
| KMS-51[b] | H | c.6297_6298delAC | p.Pro2100Glyfs*54 | Yes | Novel |
| KMS-52 | H | c.4693 + 1G > T | splice site | Yes | Novel |
| KMS-53 | H | c.10090C > T | p.Gln3364* | Yes | Novel |
| KMS-54 | T | c.8401C > T | p.Arg2801* | Yes | Novel |
| KMS-56 | H | c.15536G > A | p.Arg5179His | Yes | Ng et al. [2010] |
| KMS-58 | H | c.4333T > G | p.Cys1445Gly | Yes | Novel |
| KMS-59 | H | c.15256C > T | p.Arg5086* | Yes | Banka et al. [2012b] |
| KMS-60 | H | c.11761C > T | p.Gln3921* | Unknown | Novel |
| KMS-61[c] | W | c.5269C > T | p.Arg1757* | Yes | Novel |
| KMS-62 | H | c.15163_15168dup | p.Asp5055_Leu5056dup | Unknown[f] | Micale et al. [2011] |
| KMS-63 | T | c.4577G > T | p.Cys1526Phe | Yes | Novel |
| KMS-69 | H | c.11944C > T | p.Arg3982* | Yes | Paulussen et al. [2011] |
| KMS-70 | T | c.13903C > T | p.Gln4635* | Yes | Novel |
| KMS-71[d] | T | c.12220C > T | p.Gln4074* | Unknown | Novel |
| KMS-72 | T | c.15061C > T | p.Arg5021* | Yes | Banka et al. [2012b] |
| KMS-73 | T | c.12274C > T | p.Gln4092* | Unknown | Micale et al. [2011] |
| KMS-76 | T | c.4490_4491delAC | p.His1497Leufs*30 | Yes | Novel |
| KMS-78 | T | c.16338 + 1G > T | splice site | Yes | Novel |
| KMS-80 | T | c.15088C > T | p.Arg5030Cys | Unknown | Makrythanasis et al. [2013] |
| KMS-82 | T | c.3511G > T | p.Glu1171* | Yes | Novel |
| KMS-85 | T | c.11722C > T | p.Gln3908* | Yes | Paulussen et al. [2011] |
| KMS-87 | T | c.3281_3282delTC | p.Leu1094Profs*20 | Yes | Novel |
| KMS-88 | T | c.16052 + 1G > C | splice site | Unknown | Novel |
| KMS-91 | T | c.4267C > T | p.Arg1423Cys | Unknown | Novel |
| Patients with *KDM6A* mutations | | | | | |
| KMS-31[e] | H | c.3717G > A | p.Trp1239* | Unknown | Miyake et al. [2013] |
| KMS-37[e] | H | c.1555C > T | p.Arg519* | Unknown | Miyake et al. [2013] |
| KMS-65[e] | H | c.3354_3356delTCT | p.Leu1119del | Yes | Miyake et al. [2013] |
| KMS-81 | T | c.1909_1912delTCTA | p.Ser637Thrfs*53 | Yes | Novel |
| KMS-83 | T | c.4051C > T | p.Arg1351* | Unknown | Novel |

H, high-resolution melting analysis/Sanger sequencing; T, targeted resequencing; W, whole exome sequencing.RefSeq NM_003482.3 for *MLL2* and RefSeq NM_021140.2 for *KDM6A* were used as reference sequences.

[a]References are listed when the same mutation has been reported previously.

[b]This patient was reported as proband 1 by Tekin et al. [2006].

[c]The detailed clinical features of this patient were reported by Ito et al. [2013] because of her hypothalamic pituitary complications.

[d]The clinical course of this patient, particularly the idiopathic thrombocytopenic purpura, was reported by Torii et al. [2009].

[e]These patients have been reported in our previous study [Miyake et al., 2013].

[f]Patient KMS-62: no mutation in the mother.

TABLE II. *MLL2* Non-Truncating-Type Mutations in Patients With KS

| Amino acid change[a] | Patient ID | Domain | Polyphen-2 (score) | MutationTaster |
|---|---|---|---|---|
| p.Met1376Arg | KMS-22 | — | Probably damaging (0.915) | Polymorphism |
| p.Arg1423Cys | KMS-91 | PHD | Probably damaging (1.000) | Disease causing |
| p.Cys1445Gly | KMS-58 | PHD | Probably damaging (1.000) | Disease causing |
| p.Cys1526Phe | KMS-63 | PHD | Probably damaging (0.999) | Disease causing |
| p.Gln3277_Gln3282dup | KMS-02 | — | NA | Polymorphism |
| p.Arg5030Cys | KMS-80 | — | Probably damaging (1.000) | Disease causing |
| p.Asp5040Gly | KMS-15 | — | Probably damaging (1.000) | Disease causing |
| p.Arg5048Cys | KMS-27 | — | Probably damaging (1.000) | Disease causing |
| p.Arg5048His | KMS-38 | — | Probably damaging (1.000) | Disease causing |
| p.Asp5055_Leu5056dup | KMS-40, 62 | — | NA | Polymorphism |
| p.Arg5154Gln | KMS-23 | — | Probably damaging (1.000) | Disease causing |
| p.Arg5179His | KMS-56 | FYRN | Possibly damaging (0.840) | Disease causing |
| p.Gly5189Arg | KMS-49 | FYRN | Probably damaging (1.000) | Disease causing |
| p.Arg5351Gln | KMS-42 | — | Probably damaging (1.000) | Disease causing |

[a]The nucleotide mutation nomenclature for these predicted protein mutations are included in Table I.

and $P = 0.1778$, respectively). Blue sclera, lower lip pits, spine/rib abnormality, hip joint dislocation, umbilical hernia, kidney dysfunction, cryptorchidism, liver abnormality, spleen abnormality, premature thelarche, neonatal hyperbilirubinemia, and anemia were observed only in the mutation-positive group.

## Clinical Comparison of the *MLL2*-Mutated and *KDM6A*-Mutated Groups

We compared the clinical features between the *MLL2*-mutated and *KDM6A*-mutated groups (Figs. 3–5, Supplemental Table III). High arched eyebrows, short fifth fingers, and hypotonia in infancy were more frequent in individuals with *MLL2* mutations than in individuals with *KDM6A* mutations ($P = 0.0364$, 0.0039, and 0.0283, respectively). Short stature was more frequent in individuals with *KDM6A* mutations ($P = 0.0485$). Although not statistically significant, postnatal growth retardation was observed in all individuals with *KDM6A* mutations, whereas this was observed in only half of the individuals with *MLL2* mutations.

## Clinical Comparison of Individuals With a *MLL2* Truncating-Type and Non-Truncating-Type Mutation

Most clinical features were observed at a similar ratio in both groups (Supplemental Table IV), except for prominent ears and hypotonia, which were more frequently observed in the truncating-type group than in the non-truncating-type group ($P = 0.0339$ and $P = 0.0248$, respectively). However, the facial appearance of individuals in the truncating-type group was more typical, based on the ten originally reported patients with KS [Kuroki et al., 1981; Niikawa et al., 1981], than that in the non-truncating-type group (Figs. 3 and 4). Except for patient KMS-58, the facial appearance of patients with a non-truncating-type mutation was rather less typical. It should be noted that these patients had thick eyebrows (not present in patient KMS-56). Furthermore, ectropion of the lower eyelid, depressed nasal tip, short columella, and prominent ears all seemed less obvious in the individuals with a non-truncating-type mutation.

## X-Inactivation Pattern in Female Patients With a *KDM6A* Mutation

A *KDM6A* mutation was identified in two females (KMS-65 and KMS-81). Individual KMS-65 (c.3354_3356del, which predicts p.Leu1119del) showed a random X-inactivation pattern [Miyake et al., 2013], while individual KMS-81 with a frame-shift mutation showed marked skewing (98:2; Supplemental Fig. 1A). By RT-PCR using mRNA derived from a lymphoblastoid cell line from patient KMS-81, we confirmed that both the mutated and normal alleles were transcribed at similar levels when nonsense-mediated mRNA decay (NMD) was inhibited by cycloheximide treatment (Supplemental Fig. 1B). In untreated cells, or cells treated with dimethylsulfoxide (negative control), the mutant allele was transcribed at a lower level than the wild-type allele, indicating that NMD partially eliminated the mutant.

## Exome Sequencing

Among the five patients who were also analyzed by whole exome sequencing, mutations were identified and later confirmed by Sanger sequencing in four (Table I). Fragments with an 11 base-pair insertion (c.3326_3336dup) of *MLL2* in patient KMS-21 could not be amplified by Ex Taq, but could be amplified by LA Taq with LA buffer and confirmed by Sanger sequencing. Three other mutations were missed by HRM analysis (Table I).

## DISCUSSION

We identified 50 *MLL2* and five *KDM6A* mutations among 81 patients with KS and add to the 246 *MLL2* mutations described in patients with KS [Ng et al., 2010; Hannibal et al., 2011; Li et al., 2011; Micale et al., 2011; Paulussen et al., 2011; Banka et al., 2012a,b;


FIG. 3. Clinical features of patients with Kabuki syndrome harboring a MLL2 truncating-type mutation. A: Facial features of patients with Kabuki syndrome with a *MLL2* truncating-type mutation. The seven panels for patient KMS-54 show serial images at 0, 1, 4, 6.5, 9.5, 22, and 33 years of age, respectively. B: Complete right cleft lip/palate and lower lip pits (arrows) in patient KMS-41. C: Abnormal dentition in patients KMS-52 and KMS-59. They also showed hypodontia with wide interdentium. D: Patient KMS-72 had congenital strabismus and blepharoptosis as well as opacification of the cornea due to Peters anomaly (arrow). E: Hand images show short fifth fingers and prominent digit pads (white arrows).

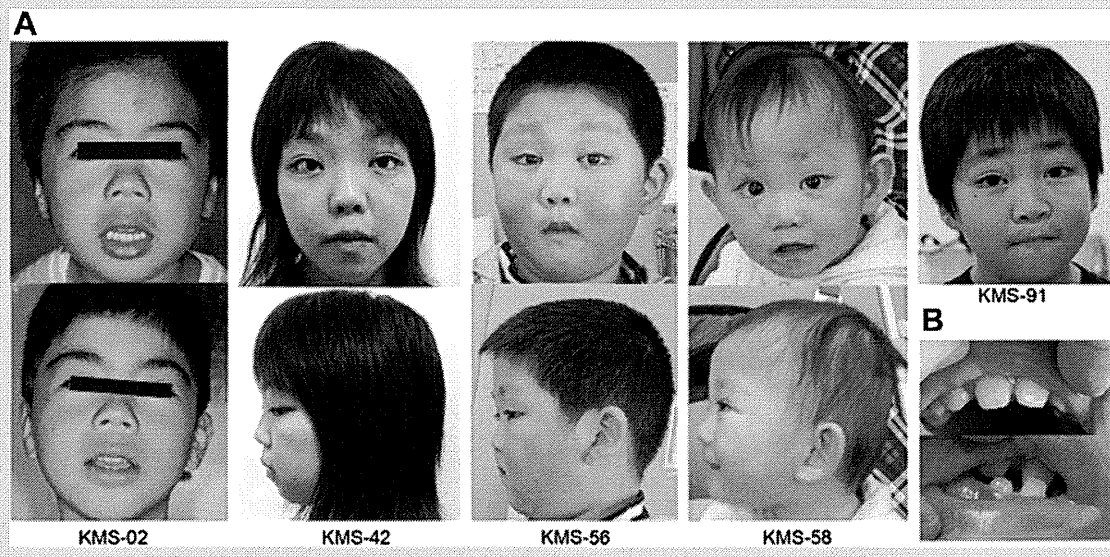


**FIG. 4. Clinical features of patients with Kabuki syndrome with a *MLL2* non-truncating-type mutation. A: Facial features of patients with KS and a *MLL2* non-truncating-type mutation. B: Patient KMS-56 showed abnormal dentition (hypodontia with wide interdentium).**

Kokitsu-Nakata et al., 2012; Tanaka et al., 2012; Bogershausen and Wollnik, 2013; Makrythanasis et al., 2013] (Human Gene Mutation Database Professional 2012.3; https://portal.biobase-international.com/hgmd/pro/gene.php). Our mutation-positivity rate for either gene was 67.9% (55/81), and that for *MLL2* only was 61.7% (50/81); these figures are compatible with those reported in a review (55–80%) [Banka et al., 2012b]. Mutation-negative patients suggest the existence of unknown genes to cause KS or misdiagnosis.

As for the phenotype–genotype relationship, Banka et al. [2012b] suggested that feeding problems, kidney anomalies, premature thelarche, joint dislocation, and palatal malformation were more frequently observed in patients with *MLL2*-mutations than in patients with normal *MLL2* sequence. Hannibal et al. [2011] reported that renal anomalies were more common in patients who had *MLL2* mutations compared to those who did not. Li et al. [2011] reported that short stature and renal anomalies were more frequent in patients with *MLL2*-mutations than in those with normal *MLL2* sequence. In our study, premature thelarche was observed only in patients with *MLL2* mutations, but this was not significant ($P = 0.1137$). The frequencies of kidney anomalies, hip joint dislocation, and short stature were not different when comparing those with and without *MLL2* mutations ($P = 0.3030$, $P = 1.0000$, and $P = 0.0717$, respectively; Supplemental Table V). High arched eyebrows, palatal malformation (cleft palate/lip), low posterior hairline, and short fifth finger were more frequently observed in individuals with *MLL2* mutations than in patients with normal *MLL2* ($P = 0.0118$, $P = 0.0284$, $P = 0.0493$, and $P = 0.0137$, respectively; Supplemental Table V).

X-inactivation skewing in patients with KS has been discussed since the discovery of the *KDM6A* deletion in a female with KS

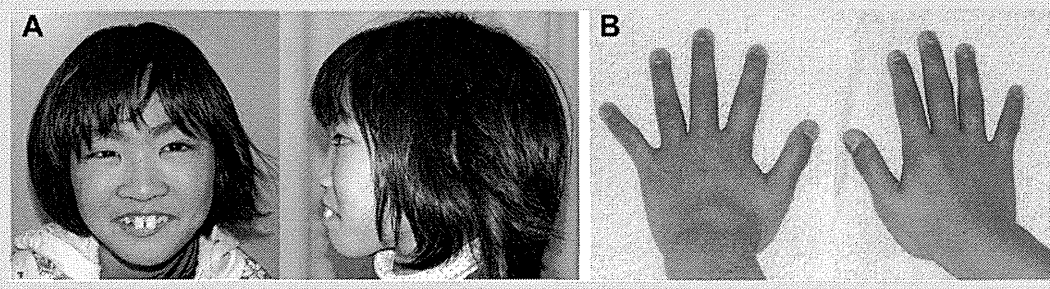


**FIG. 5. Clinical features of patients with Kabuki syndrome with a *KDM6A* truncating-type mutation. A: Facial features of patient KMS-81 harboring a *KDM6A* mutation (c.1909_1912del, p.Ser637Thrfs*53). She showed large front teeth with wide interdentium. B: Hand image of KMS-81. Short fifth finger was not remarkable.**

[Lederer et al., 2012; Miyake et al., 2013]. In two female patients reported here, patient KMS-65, who had an in-frame deletion, showed a random X-inactivation pattern, but patient KMS-81, who had a truncating-type mutation, showed marked skewing. X-inactivation skewing was also reported in two affected females with *KDM6A* deletion reported by Lederer et al. [2012]. cDNA sequence analysis of patient KMS-81 indicated that the mutant allele of *KDM6A* was expressed at a similar level to the wild-type allele under NMD inhibition. This result suggests that *KDM6A* mostly escapes X-inactivation in female lymphoblastoid cells. Interestingly, *KDM6A*/*Kdm6a* escapes X-inactivation in humans and mice, and in mice its expression level from the inactive X chromosome (Xi) was reported as 15–35% of that from the active X chromosome (Xa) [Greenfield et al., 1998; Xu et al., 2008]. We calculated the hypothetical expression assuming a 30% *KDM6A* expression level from Xi and 100% expression from Xa (Supplemental Fig. 2). In patient KMS-81, who showed marked skewing (98:2), either the mutant X chromosome or the wild-type X was inactivated in 98% of cells. If the mutant were inactivated, the expression level would be below 1 ($1.0 \times 0.98 + 0.3 \times 0.02 = 0.986$). If the wild-type were inactivated, the expression level would also be below 1 ($1.0 \times 0.02 + 0.3 \times 0.98 = 0.314$). The KS phenotype is usually unassociated with Turner syndrome (45,X), with the *KDM6A* expression level at 1.0 [Miyake et al., 2013]. It is possible that having a *KDM6A* expression level of 1.0 is essential for a normal human phenotype. Similarly, males with only one copy of *KDM6A* do not manifest KS. We previously mentioned the possibility of *UTY* compensation for *KMD6A* (Supplemental Fig. 2) [Miyake et al., 2013], although human UTY lacks demethylase activity [Hong et al., 2007; Lan et al., 2007]. The recent evidence that $X^{Utx-}X^{Utx-}$ homozygous mice demonstrated a more severe phenotype than $X^{Utx-}Y^{Uty+}$ mice indicates that UTY can compensate for the loss of UTX in embryonic development [Shpargel et al., 2012]. Because mouse and human UTY show 75% identity, and 95% identity in the Jumonji C domain [Shpargel et al., 2012], it is likely that normal human males who have only one copy of *KDM6A* are supplemented by *UTY* in a demethylase-independent manner.

Interestingly, $X^{Utx-}Y^{Uty+}$ mice showed small body size [Shpargel et al., 2012]. Similarly, the human *KDM6A*-mutated group exhibited short stature and postnatal growth retardation.

Regarding our mutation detection methods, HRM analysis and Sanger sequencing are both imperfect. Next-generation sequencing is more sensitive (especially for single nucleotide variants and small insertions/deletions), faster, and cheaper due to multiple gene screening and the potential to multiplex. However, a microdeletion involving *MLL2* or *KDM6A* or low-level mosaicism of a single nucleotide variant might be missed by this method. Therefore, in patients who test mutation-negative, more comprehensive approaches might be necessary. In conclusion, we investigated *MLL2* and *KDM6A* mutations and their clinical consequences in patients with KS. The majority of the clinical features were observed at a similar frequency among patients with either *MLL2* or *KDM6A*-mutations. The genetic basis of the patients who tested mutation-negative (20–45%) remains elusive. Further studies are necessary to understand the whole picture of the genetic aspects of KS and its genotype–phenotype relationships.

## ACKNOWLEDGMENTS

We thank the patients and their parents for participating in this work. We also thank Ms. Y. Yamashita, Ms. E. Koike, Ms. S. Sugimoto, Ms. N. Watanabe, Ms. K. Takabe, and Mr. T. Miyama for their technical assistance. This work was supported by research grants from the Ministry of Health, Labour and Welfare of Japan (H. Saitsu, N. Matsumoto, N. Miyake), the Japan Science and Technology Agency (N. Matsumoto), the Strategic Research Program for Brain Sciences (N. Matsumoto), a Grant-in-Aid for Scientific Research on Innovative Areas-(Transcription cycle)-from the Ministry of Education, Culture, Sports, Science and Technology of Japan (N. Matsumoto), a Grant-in-Aid for Scientific Research from the Japan Society for the Promotion of Science (N. Matsumoto), a Grant-in-Aid for Young Scientists from the Japan Society for the Promotion of Science (H.S., N. Miyake), the Takeda Science Foundation (N. Matsumoto, N. Miyake), the Yokohama Foundation for the Advancement of Medical Science (N. Miyake), and the Hayashi Memorial Foundation for Female Natural Scientists (N. Miyake).

## REFERENCES

Adzhubei IA, Schmidt S, Peshkin L, Ramensky VE, Gerasimova A, Bork P, Kondrashov AS, Sunyaev SR. 2010. A method and server for predicting damaging missense mutations. Nat Methods 7:248–249.

Allen RC, Zoghbi HY, Moseley AB, Rosenblatt HM, Belmont JW. 1992. Methylation of *Hpa*II and *Hha*I sites near the polymorphic CAG repeat in the human androgen-receptor gene correlates with X chromosome inactivation. Am J Hum Genet 51:1229–1239.

Banka S, Howard E, Bunstone S, Chandler K, Kerr B, Lachlan K, McKee S, Mehta S, Tavares A, Tolmie J, Donnai D. 2012a. MLL2 mosaic mutations and intragenic deletion-duplications in patients with Kabuki syndrome. Clin Genet 83:467–471.

Banka S, Veeramachaneni R, Reardon W, Howard E, Bunstone S, Ragge N, Parker MJ, Crow YJ, Kerr B, Kingston H, Metcalfe K, Chandler K, Magee A, Stewart F, McConnell VP, Donnelly DE, Berland S, Houge G, Morton JE, Oley C, Revencu N, Park SM, Davies SJ, Fry AE, Lynch SA, Gill H, Schweiger S, Lam WW, Tolmie J, Mohammed SN, Hobson E, Smith A, Blyth M, Bennett C, Vasudevan PC, Garcia-Minaur S, Henderson A, Goodship J, Wright MJ, Fisher R, Gibbons R, Price SM, CdS D, Temple IK, Collins AL, Lachlan K, Elmslie F, McEntagart M, Castle B, Clayton-Smith J, Black GC, Donnai D. 2012b. How genetically heterogeneous is Kabuki syndrome?: MLL2 testing in 116 patients, review and analyses of mutation and phenotypic spectrum. Eur J Hum Genet 20:381–388.

Bogershausen N, Wollnik B. 2013. Unmasking Kabuki syndrome. Clin Genet 83:201–211.

Dubuc AM, Remke M, Korshunov A, Northcott PA, Zhan SH, Mendez-Lago M, Kool M, Jones DT, Unterberger A, Morrissy AS, Shih D, Peacock J, Ramaswamy V, Rolider A, Wang X, Witt H, Hielscher T, Hawkins C, Vibhakar R, Croul S, Rutka JT, Weiss WA, Jones SJ, Eberhart CG, Marra MA, Pfister SM, Taylor MD. 2013. Aberrant patterns of H3K4 and H3K27 histone lysine methylation occur across subgroups in medulloblastoma. Acta Neuropathol 125:373–384.

Greenfield A, Carrel L, Pennisi D, Philippe C, Quaderi N, Siggers P, Steiner K, Tam PP, Monaco AP, Willard HF, Koopman P. 1998. The UTX gene escapes X inactivation in mice and humans. Hum Mol Genet 7:737–742.

Hannibal MC, Buckingham KJ, Ng SB, Ming JE, Beck AE, McMillin MJ, Gildersleeve HI, Bigham AW, Tabor HK, Mefford HC, Cook J, Yoshiura K, Matsumoto T, Matsumoto N, Miyake N, Tonoki H, Naritomi K,

Kaname T, Nagai T, Ohashi H, Kurosawa K, Hou JW, Ohta T, Liang D, Sudo A, Morris CA, Banka S, Black GC, Clayton-Smith J, Nickerson DA, Zackai EH, Shaikh TH, Donnai D, Niikawa N, Shendure J, Bamshad MJ. 2011. Spectrum of MLL2 (ALR) mutations in 110 cases of Kabuki syndrome. Am J Med Genet Part A 155A:1511–1516.

Hong S, Cho YW, Yu LR, Yu H, Veenstra TD, Ge K. 2007. Identification of JmjC domain-containing UTX and JMJD3 as histone H3 lysine 27 demethylases. Proc Natl Acad Sci USA 104:18439–18444.

Ito N, Ihara K, Tsutsumi Y, Miyake N, Matsumoto N, Hara T. 2013. Hypothalamic pituitary complications in Kabuki syndrome. Pituitary 16:133–138.

Kokitsu-Nakata NM, Petrin AL, Heard JP, Vendramini-Pittoli S, Henkle LE, dos Santos DV, Murray JC, Richieri-Costa A. 2012. Analysis of MLL2 gene in the first Brazilian family with Kabuki syndrome. Am J Med Genet Part A 158A:2003–2008.

Kuroki Y, Suzuki Y, Chyo H, Hata A, Matsui I. 1981. A new malformation syndrome of long palpebral fissures, large ears, depressed nasal tip, and skeletal anomalies associated with postnatal dwarfism and mental retardation. J Pediatr 99:570–573.

Lan F, Bayliss PE, Rinn JL, Whetstine JR, Wang JK, Chen S, Iwase S, Alpatov R, Issaeva I, Canaani E, Roberts TM, Chang HY, Shi Y. 2007. A histone H3 lysine 27 demethylase regulates animal posterior development. Nature 449:689–694.

Lederer D, Grisart B, Digilio MC, Benoit V, Crespin M, Ghariani SC, Maystadt I, Dallapiccola B, Verellen-Dumoulin C. 2012. Deletion of KDM6A, a histone demethylase interacting with MLL2, in three patients with Kabuki syndrome. Am J Hum Genet 90:119–124.

Lee MG, Villa R, Trojer P, Norman J, Yan KP, Reinberg D, Di Croce L, Shiekhattar R. 2007. Demethylation of H3K27 regulates polycomb recruitment and H2A ubiquitination. Science 318:447–450.

Li Y, Bogershausen N, Alanay Y, Simsek Kiper PO, Plume N, Keupp K, Pohl E, Pawlik B, Rachwalski M, Milz E, Thoenes M, Albrecht B, Prott EC, Lehmkuhler M, Demuth S, Utine GE, Boduroglu K, Frankenbusch K, Borck G, Gillessen-Kaesbach G, Yigit G, Wieczorek D, Wollnik B. 2011. A mutation screen in patients with Kabuki syndrome. Hum Genet 130:715–724.

Makrythanasis P, van Bon BW, Steehouwer M, Rodriguez-Santiago B, Simpson M, Dias P, Anderlid BM, Arts P, Bhat M, Augello B, Biamino E, Bongers EM, Del Campo M, Cordeiro I, Cueto-Gonzalez AM, Cusco I, Deshpande C, Frysira E, Louise I, Flores R, Galan E, Gener B, Gilissen C, Granneman SM, Hoyer J, Yntema HG, Kets CM, Koolen DA, Marcelis CL, Medeira A, Micale L, Mohammed S, de Munnik SA, Nordgren A, Reardon SP, Revencu N, Roscioli T, Ruiterkamp-Versteeg M, Santos HG, Schoumans J, Schuurs-Hoeijmakers JH, Silengo MC, Toledo L, Vendrell T, van der Burgt I, van Lier B, Zweier C, Reymond A, Trembath RC, Perez-Jurado L, Dupont J, de Vries BB, Brunner HG, Veltman JA, Merla G, Antonarakis SE, Hoischen A. 2013. MLL2 mutation detection in 86 patients with Kabuki syndrome: A genotype–phenotype study. Clin Genet (In Press).

Micale L, Augello B, Fusco C, Selicorni A, Loviglio MN, Silengo MC, Reymond A, Gumiero B, Zucchetti F, D'Addetta EV, Belligni E, Calcagni A, Digilio MC, Dallapiccola B, Faravelli F, Forzano F, Accadia M, Bonfante A, Clementi M, Daolio C, Douzgou S, Ferrari P, Fischetto R, Garavelli L, Lapi E, Mattina T, Melis D, Patricelli MG, Priolo M, Prontera P, Renieri A, Mencarelli MA, Scarano G, della Monica M, Toschi B, Turolla L, Vancini L, Zatterale A, Gabrielli O, Zelante L, Merla G. 2011. Mutation spectrum of MLL2 in a cohort of Kabuki syndrome patients. Orphanet J Rare Dis 6:38.

Miyake N, Mizuno S, Okamoto N, Ohashi H, Shiina M, Ogata K, Tsurusaki Y, Nakashima M, Saitsu H, Niikawa N, Matsumoto N. 2013. KDM6A point mutations cause Kabuki syndrome. Hum Mutat 34:108–110.

Ng SB, Bigham AW, Buckingham KJ, Hannibal MC, McMillin MJ, Gildersleeve HI, Beck AE, Tabor HK, Cooper GM, Mefford HC, Lee C, Turner EH, Smith JD, Rieder MJ, Yoshiura K, Matsumoto N, Ohta T, Niikawa N, Nickerson DA, Bamshad MJ, Shendure J. 2010. Exome sequencing identifies MLL2 mutations as a cause of Kabuki syndrome. Nat Genet 42:790–793.

Niikawa N, Matsuura N, Fukushima Y, Ohsawa T, Kajii T. 1981. Kabuki make-up syndrome: A syndrome of mental retardation, unusual facies, large and protruding ears, and postnatal growth deficiency. J Pediatr 99:565–569.

Niikawa N, Kuroki Y, Kajii T, Matsuura N, Ishikiriyama S, Tonoki H, Ishikawa N, Yamada Y, Fujita M, Umemoto H, Iwama Y, Kondoh I, Fukushima Y, Nako Y, Matsui I, Urakami T, Aritaki S, Hara M, Suzuki Y, Chyo H, Sugio Y, Hasegawa T, Yamanaka T, Tsukino R, Yoshida A, Nomoto N, Kawahito S, Aihara R, Toyota S, Ieshima A, Funaki H, Ishitobi K, Ogura S, Furumae T, Yoshino M, Tsuji Y, Kondoh T, Matsumoto T, Abe K, Harada N, Miike T, Ohdo S, Naritomi K, Abushwereb AK, Braun OH, Schmid E. 1988. Kabuki make-up (Niikawa–Kuroki) syndrome: A study of 62 patients. Am J Med Genet 31:565–589.

Paulussen AD, Stegmann AP, Blok MJ, Tserpelis D, Posma-Velter C, Detisch Y, Smeets EE, Wagemans A, Schrander JJ, van den Boogaard MJ, van der Smagt J, van Haeringen A, Stolte-Dijkstra I, Kerstjens-Frederikse WS, Mancini GM, Wessels MW, Hennekam RC, Vreeburg M, Geraedts J, de Ravel T, Fryns JP, Smeets HJ, Devriendt K, Schrander-Stumpel CT. 2011. MLL2 mutation spectrum in 45 patients with Kabuki syndrome. Hum Mutat 32:E2018–E2025.

Prasad R, Zhadanov AB, Sedkov Y, Bullrich F, Druck T, Rallapalli R, Yano T, Alder H, Croce CM, Huebner K, Mazo A, Canaani E. 1997. Structure and expression pattern of human ALR, a novel gene with strong homology to ALL-1 involved in acute leukemia and to Drosophila trithorax. Oncogene 15:549–560.

Schuettengruber B, Chourrout D, Vervoort M, Leblanc B, Cavalli G. 2007. Genome regulation by polycomb and trithorax proteins. Cell 128:735–745.

Schwarz JM, Rodelsperger C, Schuelke M, Seelow D. 2010. MutationTaster evaluates disease-causing potential of sequence alterations. Nat Methods 7:575–576.

Shpargel KB, Sengoku T, Yokoyama S, Magnuson T. 2012. UTX and UTY demonstrate histone demethylase-independent function in mouse embryonic development. PLoS Genet 8:e1002964.

Tanaka R, Takenouchi T, Uchida K, Sato T, Fukushima H, Yoshihashi H, Takahashi T, Tsubota K, Kosaki K. 2012. Congenital corneal staphyloma as a complication of Kabuki syndrome. Am J Med Genet Part A 158A:2000–2002.

Tekin M, Fitoz S, Arici S, Cetinkaya E, Incesulu A. 2006. Niikawa–Kuroki (Kabuki) syndrome with congenital sensorineural deafness: Evidence for a wide spectrum of inner ear abnormalities. Int J Pediatr Otorhinolaryngol 70:885–889.

Torii Y, Yagasaki H, Tanaka H, Mizuno S, Nishio N, Muramatsu H, Hama A, Takahashi Y, Kojima S. 2009. Successful treatment with rituximab of refractory idiopathic thrombocytopenic purpura in a patient with Kabuki syndrome. Int J Hematol 90:174–176.

Tsurusaki Y, Kobayashi Y, Hisano M, Ito S, Doi H, Nakashima M, Saitsu H, Matsumoto N, Miyake N. 2013. The diagnostic utility of exome sequencing in Joubert syndrome and related disorders. J Hum Genet 58:113–115.

Xu J, Deng X, Watkins R, Disteche CM. 2008. Sex-specific differences in expression of histone demethylases Utx and Uty in mouse brain and neurons. J Neurosci 28:4521–4527.

# Malfunction of Nuclease ERCC1-XPF Results in Diverse Clinical Manifestations and Causes Cockayne Syndrome, Xeroderma Pigmentosum, and Fanconi Anemia

Kazuya Kashiyama,[1,2,3,16] Yuka Nakazawa,[2,4,16] Daniela T. Pilz,[5,16] Chaowan Guo,[2,4,16] Mayuko Shimada,[2,4] Kensaku Sasaki,[2,4] Heather Fawcett,[6] Jonathan F. Wing,[6] Susan O. Lewin,[7] Lucinda Carr,[8] Tao-Sheng Li,[9] Koh-ichiro Yoshiura,[10] Atsushi Utani,[11] Akiyoshi Hirano,[1] Shunichi Yamashita,[3,12] Danielle Greenblatt,[13] Tiziana Nardo,[14] Miria Stefanini,[14] David McGibbon,[13] Robert Sarkany,[13] Hiva Fassihi,[13] Yoshito Takahashi,[15] Yuji Nagayama,[4] Norisato Mitsutake,[2,3] Alan R. Lehmann,[6,17,*] and Tomoo Ogi[2,4,17,*]

Cockayne syndrome (CS) is a genetic disorder characterized by developmental abnormalities and photodermatosis resulting from the lack of transcription-coupled nucleotide excision repair, which is responsible for the removal of photodamage from actively transcribed genes. To date, all identified causative mutations for CS have been in the two known CS-associated genes, *ERCC8* (*CSA*) and *ERCC6* (*CSB*). For the rare combined xeroderma pigmentosum (XP) and CS phenotype, all identified mutations are in three of the XP-associated genes, *ERCC3* (*XPB*), *ERCC2* (*XPD*), and *ERCC5* (*XPG*). In a previous report, we identified several CS cases who did not have mutations in any of these genes. In this paper, we describe three CS individuals deficient in *ERCC1* or *ERCC4* (*XPF*). Remarkably, one of these individuals with XP complementation group F (XP-F) had clinical features of three different DNA-repair disorders—CS, XP, and Fanconi anemia (FA). Our results, together with those from Bogliolo et al., who describe XPF alterations resulting in FA alone, indicate a multifunctional role for XPF.

Cockayne syndrome (CS [MIM 216400 and 133540]) is a rare autosomal-recessive disorder characterized by growth retardation, microcephaly, impairment of nervous system development, pigmentary retinopathy, peculiar facies, and progeria together with abnormal skin photosensitivity.[1] On the basis of its clinical severity, CS is classified into three types: (1) CS type I, the classical (moderate) form, which is characterized by normal prenatal growth and the onset of progressive developmental abnormalities in infancy; (2) CS type II, the more severe (early-onset) form, in which prenatal developmental abnormalities are present; and (3) CS type III, a milder form in which progeroid symptoms manifest after middle age (see GeneReview in Web Resources). CS type II is often considered for differential diagnoses of other microcephalic maldevelopmental disorders, such as cerebrooculofacialskeletal syndrome (COFS [MIM 214150], also known as Pena-Shokeir syndrome type II) and Warburg Micro syndrome (MIM 600118).[2] In addition to these CS classes, there are rare CS variants that display the combined features of CS and XP (MIM 278700, 610651, 278720, 278730, 278740, 278760, and 278780), termed XPCS. Although CS is commonly associated with sunlight sensitivity, the dermatological phenotypes in CS are milder than those in XP and skin cancers are not found in CS. XPCS individuals, however, present with severe skin phenotypes, including severe photosensitivity, abnormal skin pigmentation, and skin cancer predisposition, all of which are common to XP individuals, who also show developmental abnormalities typical of CS.

XP and CS are associated with deficiencies in nucleotide excision repair (NER), which removes sunlight-induced UV photolesions and bulky DNA base adducts from cellular DNA.[3] NER is subdivided into two pathways, global genome NER (GG-NER) and transcription-coupled NER (TC-NER), which are distinct in their initial DNA-damage recognition processes. In contrast to XPCS, which causes defects in both pathways, CS causes specific defects to TC-NER.[4] To date, all CS (types I, II, and III)-affected individuals have been associated with mutations in *ERCC8*

[1]Department of Plastic and Reconstructive Surgery, Graduate School of Biomedical Sciences, Nagasaki University, 1-7-1 Sakamoto, Nagasaki 852-8501, Japan; [2]Nagasaki University Research Centre for Genomic Instability and Carcinogenesis, Nagasaki University, 1-12-4 Sakamoto, Nagasaki 852-8523, Japan; [3]Department of Radiation Medical Sciences, Atomic Bomb Disease Institute, Nagasaki University, 1-12-4 Sakamoto, Nagasaki 852-8523, Japan; [4]Department of Molecular Medicine, Atomic Bomb Disease Institute, Nagasaki University, 1-12-4 Sakamoto, Nagasaki 852-8523, Japan; [5]Institute of Medical Genetics, University Hospital of Wales, Cardiff CF14 4XW, UK; [6]Genome Damage and Stability Centre, University of Sussex, Falmer, Brighton BN1 9RQ, UK; [7]Division of Medical Genetics, Department of Pediatrics, University of Utah, Salt Lake City, UT 84132, USA; [8]Great Ormond Street Hospital for Children, London WC1N 3HJ, UK; [9]Department of Stem Cell Biology, Atomic Bomb Disease Institute, Nagasaki University, 1-12-4 Sakamoto, Nagasaki 852-8523, Japan; [10]Department of Human Genetics, Atomic Bomb Disease Institute, Nagasaki University, 1-12-4 Sakamoto, Nagasaki 852-8523, Japan; [11]Department of Dermatology, Graduate School of Biomedical Sciences, Nagasaki University, 1-12-4 Sakamoto, Nagasaki 852-8523, Japan; [12]Fukushima Medical University, Fukushima 960-1295, Japan; [13]UK National Xeroderma Pigmentosum Service, Department of Photodermatology, St. John's Institute of Dermatology, St. Thomas's Hospital, London SE1 7EH, UK; [14]Istituto di Genetica Molecolare, Consiglio Nazionale delle Ricerche, Pavia 27100, Italy; [15]Innovative Beauty Science Laboratory, Kanebo Cosmetics Inc., Odawara 250-0002, Japan
[16]These authors contributed equally to this work
[17]These authors contributed equally to this work
*Correspondence: togi@nagasaki-u.ac.jp (T.O.), a.r.lehmann@sussex.ac.uk (A.R.L.)
http://dx.doi.org/10.1016/j.ajhg.2013.04.007. 

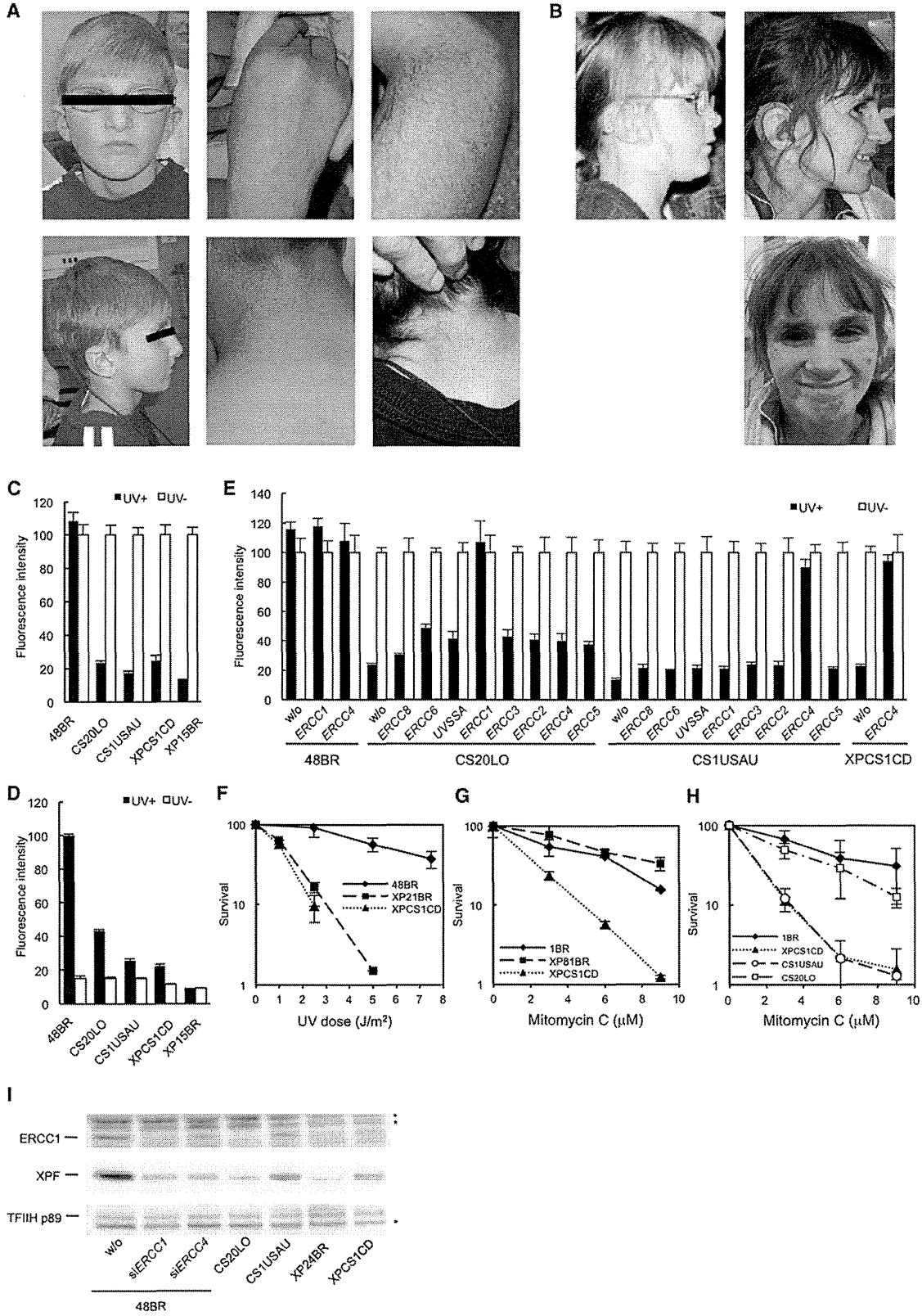


**Figure 1. Three CS Individuals Belong to the ERCC1 and XP-F Complementation Groups**

(A) CS1USAU, aged 8 years (left and middle panels) and 16 years (right panels). Note the pigmentation and hypopigmented maculas.

(B) XPCS1CD with features of XP, CS, and FA at 7.5 (left) and 11 years old (right).

(C) Reduction of RRS rates after UV irradiation in three CS cell lines (filled bars, 11 J/m$^2$ UVC; empty bars, no UV). RRS was measured by ethynyluridine (EU) incorporation and nuclear fluorescence detection (EU assay). 48BR is a normal control, CS20LO, CS1USAU, and XPCS1CD are CS cells, and XP15BR is affected by XP complementation group A (XP-A).

(D) Reduced level of unscheduled DNA synthesis (UDS) in the CS cells (filled bars, 20 J/m$^2$ UVC; empty bars, no UV).

*(legend continued on next page)*

(*CSA*) or *ERCC6* (*CSB*),[5] the products of which function, together with UVSSA (the product of the gene defective in UV-sensitive syndrome 3 [UVSS3 (MIM 614640), also known as UVSS-A])[6–8] in the still poorly understood initiation reaction of TC-NER, namely, the processing of the elongating form of RNA polymerase II stalled at the site of UV-induced DNA damage. These products thereby facilitate further recruitment of TFIIH, XPA, and NER incision endonucleases, ERCC1-XPF (ERCC4) and XPG (ERCC5), to carry out the removal of photolesions from actively transcribed genes.[4] In contrast to TC-NER, GG-NER is a genome-wide repair mechanism, and it shares the later steps with TC-NER and is deficient in several types of XP and XPCS.

The lack of TC-NER, as found in CS, can be assessed by a deficiency in the RRS test, which measures the recovery of RNA synthesis after UV irradiation. Another marker for DNA repair activity, the unscheduled DNA synthesis (UDS) test measures the GG-NER activity as the level of dNTP incorporation during DNA-repair synthesis after UV damage. Being negative for RRS and positive for UDS is diagnostic for CS. We have developed an efficient system for measuring RRS and UDS activities by using the incorporation of ethynyluracil derivatives and automated fluorescence-based imaging.[9,10] In a previous report, we sequenced all coding exons and their neighboring exon-intron boundaries of *ERCC8*, *ERCC6*, and *UVSSA* of 61 CS individuals whose genetic and/or molecular defects had not yet been determined so that we could evaluate whether *UVSSA* mutations might also result in CS phenotypes.[6] Although we did not identify any CS pathogenic mutation in *UVSSA*, we did identify several CS individuals who did not appear to have any causal mutations in *ERCC8*, *ERCC6*, or *UVSSA*, suggesting that additional gene(s) involved in TC-NER remain to be discovered.

Here, we report on three CS individuals who have normal *ERCC8* and *ERCC6* but have a defect in either *ERCC1* or *ERCC4* (*XPF*). In two cases, the affected individuals displayed typical CS clinical features (CS types I and II). In the third case, the affected individual not only had the combined XPCS phenotype but also had features of a third DNA-repair disorder, Fanconi anemia (FA [MIM 227650]). We propose that *ERCC1* and *ERCC4* be included as CS- and FA-associated genes.

CS20LO (photographs unavailable) was the daughter of nonconsanguineous parents and had an uneventful antenatal period. At 4–6 months of age, she had microcephaly, micrognathia, and contractures in the knees and elbows and was hypertonic with a dislocated radial head, deep-set eyes, and several moderate skeletal abnormalities, including camptodactyly, adducted thumbs, stiff limbs, steeply sloping acetabulae, wrist contracture, slender long bones with mildly flared metaphyses, and moderate kyphoscoliosis. She displayed brisk reflexes, and there were no feeding concerns. The karyotype was normal. Brain MRI at birth indicated a possible polymicrogyria; a nuclear-magnetic-resonance scan when she was 4 months old revealed large (>2 cm in depth) bilateral subdurals but no major visible malformations. An abnormal electroencephalogram was noticed at 9 months of age. At 16 months of age, she had nystagmus but no additional ophthalmic abnormalities; her corneas were completely clear and showed no evidence of cataracts. The diagnosis was confirmed as CS type II (early onset) because of RRS deficiency (see below). She died at the age of 2.5 years.

CS1USAU (Figure 1A) was born at around 41 weeks with a birth weight of 2.9 kg. He was prenatally diagnosed with microcephaly. His head circumference was at about the 9$^{th}$ percentile in the first few months and was lower than the 2$^{nd}$ percentile by 1 year of age. He developed normally for the first year without obvious abnormalities, except for the microcephaly. At the age of 5 years, he developed multiple unusual plantar warts on his hands and forearms. He had unusual freckling on his hands and the back of his neck and tended to burn easily and quickly, but did not blister badly, when he was exposed to sunlight. Since then, he has been well protected from solar exposure. At 7 years of age, he had deep-set eyes, progressive scoliosis, and multiple contractures in his feet; he required lengthening of the Achilles tendon because of muscle cramps in his hamstrings and calves. His skin was deeply pigmented with rashes and flat freckles. He displayed moderate bilateral hearing impairment, especially in the higher tones (he had normal hearing before the age of 3 years), short stature (height of 110.4 cm [<2$^{nd}$ percentile] and weight of 16.3 kg [<3$^{rd}$ percentile]), microcephaly (head circumference of 45.5 cm [<2$^{nd}$ percentile]), and circulatory problems. He had bilateral astigmatism but no cataracts,

(E) Complete rescue of the RRS deficiency by the infection of recombinant lentivirus expressing *ERCC1* cDNA in CS20LO cells and *ERCC4* cDNA in CS1USAU and XPCS1CD cells (filled bars, 10 J/m$^2$ UVC; empty bars, no UV).
(F) The colony-forming ability of XPCS1CD cells after UVC irradiation was compared with that of a normal control (48BR) and that of a cell strain with XP complementation group C (XP21BR).
(G) The colony-forming ability of XPCS1CD cells was compared with that of a normal control (1BR) and that of an XP-A cell strain (XP81BR) after treatment with different doses of mitomycin C (MMC) for 10 min.
(H) MMC sensitivity of different cell strains was determined by MMC treatment for 10 min and measurement of their viability by their ability to incorporate $^3$H-thymidine (5 μCi/ml; 3 hr incubation) 3 days after treatment.
(I) Immunoblotting of ERCC1 and XPF in cells from CS individuals, *ERCC4*-deficient XP24BR cells, and normal 48BR cells with the TFIIH-p89 (XPB) subunit as a loading control. 48BR cells were mock transfected or transfected with siRNAs targeting either *ERCC1* or *ERCC4*. Asterisks indicate nonspecific bands. RRS was normalized to activity in nonirradiated cells. UDS activity was normalized to that of normal 48BR cells.
Error bars represent the SD of medians of nuclear fluorescence measurements in quintuplicate samples in (C)–(E) and the SD of means of triplicate experiments in (F)–(H).

attention deficit hyperactivity disorder, and learning disability. There were no obvious abnormalities apart from some delayed myelination on brain MRI at the age of 3 years, although basal ganglia T1 shortening was observed at the age of 7 years. He had severe migraines and headaches. His ambulation lessened over time, and he needed a gastrostomy-jejunostomy tube for feeding. Diagnosis of CS was confirmed at the age of 7 years because of RRS deficiency (see below). He is currently 16 years old.

XPCS1CD (Figure 1B) was the second child of nonconsanguineous parents. Intrauterine growth failure was noted during pregnancy, and therefore labor was induced at 38 weeks. Her birth weight was between the $0.4^{th}$ and $2^{nd}$ percentiles, her developmental milestones were globally delayed, and she required speech therapy. By 18 months of age, she was reported to sunburn with minimal sun exposure in both winter and summer months in the UK. Her parents described that sunburns would develop 24 hr after exposure, peak at 2–3 days, and resolve after 10–14 days. As a result, she was carefully photoprotected and did not have any further sunburn reactions after 4 years of age. When she was 5 years old, she developed progressive bilateral sensorineural deafness, and 2 years later, she presented with worsening ataxia, tremor, and weakness. She had short stature and significant microcephaly. At the age of 7.5 years (Figure 1B, left), her height was 1.4 cm below the $0.4^{th}$ percentile and her occipitofrontal head circumference (OFC) was 6.5 cm below the $0.4^{th}$ percentile. By the age of 6 years, she was thrombocytopenic and neutropenic, coinciding with treatment for recurrent infections. Her blood film showed irregularly shaped cells, and she gradually became pancytopenic with transfusion dependence by the age of 9 years. Renal impairment was detected at the age of 10 years, when she presented with hypertension, nephrotic range proteinuria, and rising serum creatinine. The karyotype was normal.

Upon examination at 11 years of age (Figure 1B, right), she was microcephalic with an OFC well below the $0.4^{th}$ percentile and had extremely short stature. She had deep-set eyes, a prominent nose, small teeth, and freckling over the nose and cheeks. There was marked palmar erythema, and extensive plane warts were seen on the arms. Her skin had an aged appearance, particularly over the dorsal hands. She had five café-au-lait macules. Her neurological examination highlighted a resting tremor, head titubation, and an ataxic gait. She demonstrated saccadic eye movements and an element of vertical nystagmus. There was subtle pyramidal tract weakness distally with extensor plantar reflexes. Sensation was intact. Ophthalmological examination revealed hypermetropia and bilateral blepharitis, but no other ocular abnormalities. MRI of the brain showed increased signal in the peritrigonal white-matter bilaterally. A renal biopsy and bone marrow aspirate were performed under general anesthesia (when she was 11 years old). The bone marrow showed a profoundly hypocellular sample in which all three lineages were present, blast percentage was <1%, and dysplasia was minimal. No clonal cytogenetic abnormalities were detected. A simultaneous full blood count showed a haemoglobin level of 9.4 g/dl (11.5–15.5 g/dl), a red blood cell count of $2.98 \times 10^{12}$/l ($3.40–5.20 \times 10^{12}$/l), and a mean corpuscular volume of 95.0 fl (80.0–98.0 fl). Studies of liver function were normal. The renal biopsy showed areas of focal segmental glomerular sclerosis and evident thickening of the capillary basement membrane. There was a background of interstitial fibrosis and tubular atrophy with glomerular shrinkage. She died at the age of 12 years after acute deterioration of her renal function. A postmortem examination was not done.

Many of her features were characteristic of CS,[11] although pancytopenia and renal failure are not usually associated with this disorder. The exaggerated and prolonged sunburn reactions together with progressive freckling at sun-exposed sites were suggestive of XP, whereas the pancytopenia, bone marrow findings, and recurrent infections are features often seen in FA.

To determine DNA-repair activities in the CS individuals' cells, we established dermal fibroblast cultures from skin biopsies. Written informed consent was obtained from the individuals' families, and the experiments were carried out in accordance with the local ethical standards (Nagasaki University Ethical, Legal, and Social Implications committee). We first measured the RRS rate after exposure to 10 J/m$^2$ UVC irradiation.[6,9,10] RNA-synthesis activity was significantly reduced in all three CS cell lines compared with normal cells (Figure 1C), indicating a deficiency in TC-NER activity, as expected for CS cells. We also measured UDS, a mark of GG-NER activity,[6,9,10] which is not normally affected in CS cells.[12] We found a significant reduction in UDS rates in all three CS cell lines (Figure 1D). These results imply that the CS individuals have defective GG-NER and TC-NER pathways, and we therefore presumed that, unlike other CS individuals, they carry defects in genes that commonly function in both the TC-NER and GG-NER pathways. Consequently, we anticipated that these three CS individuals might carry mutations either in *ERCC3* (*XPB*), *ERCC2* (*XPD*), *ERCC4*, or *ERCC5* (*XPG*) or in *ERCC1*, and we assayed complementation of the RRS defects by infecting the CS cells lines with recombinant lentiviruses expressing one of these NER-related cDNAs[6] (Figure 1E). The RRS defects were dramatically and specifically restored when CS20LO cells were infected with lentiviruses expressing *ERCC1* and when CS1USAU and XPCS1CD cells were infected with *ERCC4* cDNA, but not when the cells were infected with other viruses (Figure 1E). We conclude that CS20LO is assigned to the ERCC1 complementation group and that, likewise, CS1USAU and XPCS1CD are assigned to XP complementation group F (XP-F).

A hallmark of cells from individuals with FA is a specific defect in the repair of DNA interstrand crosslinks (ICLs). The ERCC1-XPF complex, which is uniquely among the NER proteins, is also involved in ICL repair.[13,14] Because several clinical features of XPCS1CD are characteristic of

FA, we measured the survival of this individual's cells after exposure to UV irradiation and to the crosslinking agent mitomycin C (MMC). Figure 1F shows that cells from XPCS1CD are as sensitive to UV irradiation as those from an XP control. In contrast, the XP control cells (in this case, from group A) are, as reported in the literature,[15] not sensitive to MMC, whereas XPCS1CD cells are much more sensitive (Figure 1G). Furthermore, chromosome-breakage studies on blood showed increased sensitivity to MMC and an elevated level of chromosome damage upon exposure to the alkylating agent DEB (1,2,3,4-diepoxybutane). However, the levels were lower than expected for a diagnosis of FA (data not shown). In view of these observations, we also examined the MMC sensitivity of CS1USAU and CS20LO cells and found that the former were also very sensitive to MMC, whereas the latter were marginally, if at all, sensitive (Figure 1H).

ERCC1 is needed for stabilizing and enhancing XPF endonuclease activity,[16,17] and indeed, using immunoblotting, we observed a significant reduction in the expression level of XPF concurrently with the reduction of ERCC1 expression in CS20LO cells (Figure 1I). In contrast, XPF and ERCC1 levels were modestly reduced in CS1USAU and XPCS1CD cells (Figure 1I).

To determine the genetic changes in the three CS individuals, we carried out (1) PCR-based gDNA amplification of the exons and neighboring exon-intron boundaries of *ERCC1* from CS20LO cells and of *ERCC4* from CS1USAU cells and subsequent direct sequencing of the amplified gDNA fragments and (2) RT-PCR of mRNA and sequencing of the cDNA from XPCS1CD cells. In CS20LO cells, a homozygous mutation, c.693C>G, in exon 7 of *ERCC1* (RefSeq accession number NM_001983.3) resulted in amino acid substitution p.Phe231Leu, located in the C-terminal XPF-interacting helix-hairpin-helix (HhH) domain (Figure 2A). ERCC1 pathogenic changes identified in NER-deficient diseases and in other genetic disorders are extremely rare; only two cases have been reported.[18,21] Individual 165TOR,[21] who had clinical features overlapping those of CS and was diagnosed with a severe form of COFS, was heterozygous for the *ERCC1* c.693C>G (p.Phe231Leu) mutation found in our CS individual. In 165TOR, the other *ERCC1* pathogenic allele was c.472C>T (p.Gln158*); however, the mutated transcript is presumed to be subject to nonsense-mediated mRNA decay (NMD). XP202DC[18] was a XP individual who developed progressive neurodegeneration during adolescence and died at the age of 37 years. He was compound heterozygous for nonsense substitution p.Lys226* near the C terminus and splice-site mutation c.604-26G>A, which might have affected the expression level of wild-type ERCC1. In this individual, a low amount of the wild-type *ERCC1* allele expression might have been sufficient to ameliorate the more severe aspects of the disorder.

CS1USAU cells had two heterozygous mutational changes in *ERCC4* (RefSeq NM_005236.2): (1) an exon 4 mutation, c.706T>C, causing an amino acid substitution, p.Cys236Arg, located in the N-terminal large SF2 helicase domain and (2) an exon 8 frameshift insertion, c.1730_1731insA, which generated a premature stop codon, p.Tyr577* (Figure 2B). XPCS1CD had two *ERCC4* heterozygous mutations, c.706T>C and c.1765C>T, resulting in changes p.Cys236Arg (the same mutation as we found in CS1USAU) and p.Arg589Trp (previously found in three XP individuals) (Figure 2C), respectively.[18] Previously identified alterations in ERCC1 and XPF, together with those identified in this paper, are shown in Figure 2D.

XPF pathogenic alterations are normally associated with mild XP cases without severe developmental abnormalities.[18] There has been one exceptional case, XFE progeroid syndrome (MIM 610965). The affected individual, XP51RO, carried a homozygous mutation resulting in a p.Arg153Pro change in the SF2 domain of XPF.[22] In all reported cases with mild XP-F, the pathogenic mutations are hypomorphic and there is a substantial amount of residual XPF in the cells; however, in the XFE individual cells, XPF expression was severely reduced.[22] In contrast, in CS1USAU and XPCS1CD cells, a substantial amount of XPF remained (Figure 1I), suggesting that the pathogenic allele is fully expressed and the altered protein is stable (also see later purification of the ERCC1-XPF complex). These observations indicate that p.Cys236Arg causes XPF dysfunction and confers a CS phenotype on individuals CS1USAU and XPCS1CD.

XPF and ERCC1 form a heterodimeric structure-specific endonuclease, the ERCC1-XPF complex, which cleaves on the 5′ side of the UV-damaged DNA at the incision step of NER.[23–25] The proteins form a complex through their C-terminal HhH domains and stabilize the counterpart when in a complex. To test whether the p.Phe231Leu altered ERCC1 and the p.Cys236Arg altered XPF form proper ERCC1-XPF complexes, we introduced the altered proteins (V5-tagged) into 293FT cells and performed immunoprecipitation to check the binding affinity between ERCC1 and XPF. Although the ERCC1 p.Phe231Leu substitution is located in the XPF-binding HhH domain and the residue interfaces with two alpha helices of the XPF HhH domain, the altered ERCC1 binding capacity to XPF was unaffected by the substitution (Figure 3A). Similarly, we observed no significant decrease in coprecipitation of wild-type ERCC1 in the complex when p.Cys236Arg XPF was expressed (Figure 3B). The ERCC1-XPF complex also interacts with TFIIH, as shown by both in vitro and in vivo experiments.[26] We therefore tested the binding affinity of altered ERCC1 and XPF with the XPB-p89 subunit of TFIIH. Although there was no significant reduction in binding affinity of p.Phe231Leu ERCC1 expressed in 293FT cells (Figure 3A), we observed, after UV irradiation, less p89 in immunoprecipitates from cells expressing p.Cys236Arg XPF than from wild-type controls (Figure 3B). Recent studies also demonstrated that the three known structure-specific endonuclease complexes (SSEs)—ERCC1-XPF, SLX4 (FANCP)-SLX1, and MUS81 (SLX3)-EME1 (SLX2)—interact with each other in

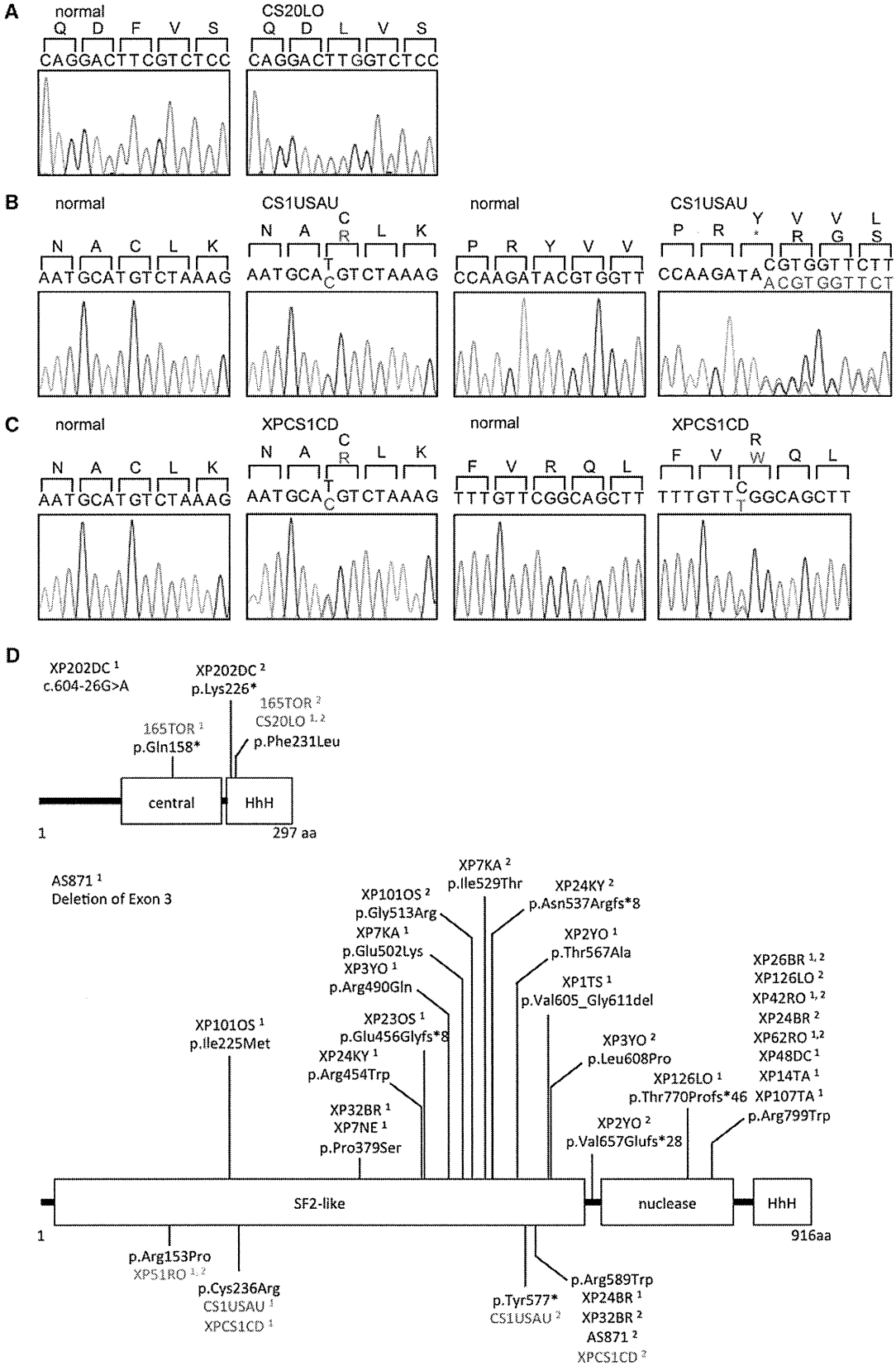


**Figure 2. Locations of the *ERCC1* and *ERCC4* Mutations Identified in the CS Cells and in Known NER Disorders**
(A) The homozygous c.693C>G single-nucleotide variant (SNV) in *ERCC1* exon 7 in the CS individual, CS20LO; the altered amino acid, Phe231, is shown in red.
(B) The heterozygous c.706T>C SNV in *ERCC4* exon 4 and the 1 base insertion, c.1730_1731insA, in *ERCC4* exon 8 are identified in the CS individual, CS1USAU. The altered amino acids, Cys236 and Tyr577, are shown in red.

*(legend continued on next page)*

crosslink-repair pathways. Importantly, mutations in *SLX4* have been identified in several FA individuals, and SLX4 acts as a scaffold and plays a key role in the coordination of these interactions.[27–29] We therefore tested whether one of these interactions, namely the binding affinity of the altered protein with MUS81 (Figure 3B), is compromised in cells expressing the XPF p.Cys236Arg substitution. There was no impact on the binding affinity, suggesting that this was not the cause of the FA features observed in XPCS1CD.

To further test whether the altered ERCC1 and XPF proteins retain any DNA-repair functions, we performed complementation analyses of the RRS defects by expressing mutant *ERCC1* and *ERCC4* cDNAs in the ERCC1- and XPF-deficient CS cells, respectively (Figure 3C). Consistent with the previous report describing a correction of UV sensitivity after transfection with the *ERCC1* c.693C>G (p.Phe231Leu) pathogenic mutant cDNA into ERCC1-deficient 165TOR cells,[21] we observed that RRS in the ERCC1-deficient CS20LO cells was fully restored upon infection with the lentivirus expressing c.693C>G (p.Phe231Leu) mutant *ERCC1* cDNA, whereas expression of the p.Cys236Arg altered XPF failed to restore RRS levels of the XPF-deficient CS1USAU cells.

We then purified recombinant ERCC1-XPF complexes and determined their endonuclease activity. As observed in Figure 1I, the altered p.Cys236Arg XPF complex was stable (Figure 3D). Because stem-loop structures are good substrates for the ERCC1-XPF complex,[30] we performed in vitro incision assays with fluorescent-labeled DNA templates containing a 12 bp stem-dT22-loop.[19,30] We observed significant reduction of the endonuclease activity of the p.Cys236Arg altered complex (Figure 3E).

These data indicate that XPF malfunction, caused by the lack of proper interaction between TFIIH and ERCC1-XPF, and a substantial reduction of the stem-loop incision activity of the endonuclease complex cause the CS and FA phenotypes in CS1USAU and XPCS1CD, whereas the reason for ERCC1 deficiency in CS20LO cells remains unclear.

Unlike NER-associated genes that are responsible exclusively for CS and UVSS phenotypes (i.e., *ERCC8*, *ERCC6*, and *UVSSA*), *ERCC4* and *ERCC1* are presumably indispensable for fetal development because there is no known individual carrying homozygous or compound-heterozygous null mutations in either of the genes. Given that we found that the p.Phe231Leu altered ERCC1 retains normal NER function, we decided to determine the precise expression levels of the mutant *ERCC1* and *ERCC4* alleles identified in two of the CS individuals. We undertook allele-specific quantitative RT-PCR (qRT-PCR) with sets of primers that selectively amplify the wild-type or the mutant *ERCC1* and *ERCC4* cDNAs (Table 1). In CS20LO cells, primer set ERCC1-WT and ERCC1-Rv1 allowed specific amplification of the wild-type *ERCC1* allele (Figure 4A, left), whereas another set of primers, ERCC1-p.Phe231Leu and ERCC1-Rv1, amplified the c.693C>G (p.Phe231Leu) allele in exon 7 (Figure 4A, middle); primers ERCC1-com1 and ERCC1-Rv1 amplified both the wild-type and the mutant alleles (Figure 4A, right). We observed a very low level (50-fold < wild-type) of expression of the *ERCC1* c.693C>G (p.Phe231Leu) allele in CS20LO cells (Figure 4A, middle and right), suggesting that the ERCC1-null phenotype can be ascribed to this drastic attenuation of *ERCC1* mRNA expression. Subsequently, expression of the wild-type and the two mutated *ERCC4* alleles in CS1USAU cells was examined. Similarly to how we quantified *ERCC1* mRNA, we designed sets of primers to specifically amplify the c.706T>C (p.Cys236Arg) allele located in exon 4 (Figure 4B, middle) and the c.1730_1731insA (p.Tyr577*) allele in exon 8 (Figure 4C, middle), as well as their corresponding wild-type alleles (Figure 4B and 4C, left). We confirmed the expression of the c.706T>C (p.Cys236Arg) allele specifically in CS1USAU cells (Figure 4B, middle and right) with primers XPF-p.Cys236Arg and XPF-Rv1, whereas the c.1730_1731insA (p.Tyr577*) allele, measured by primers XPF-p.Tyr577* and XPF-Rv2, was subjected to NMD, because its expression level was very low in the CS cells (Figure 4C, middle). Given these qRT-PCR data and the protein expression levels in the CS cells (Figure 1I), we conclude that the ERCC1-deficiency phenotype in CS20LO results from a very low level of expression of the mutant allele and that the XPF deficiency in CS1USAU and XPCS1CD is mainly caused by protein malfunction. A summary of our findings is presented in Table 2.

We have identified three CS individuals who carry pathogenic mutations in either *ERCC1* or *ERCC4*. Approximately 25 XP-F individuals have been described in the literature.[18] The majority of them are XP individuals, who, compared with individuals affected by XP complementation group C, have relatively mild skin problems and skin cancers that appear relatively later in life. Only XFE individual XP51RO had a much more severe phenotype.[22] Like our CS individuals, he had short stature, cachexia, and microcephaly. He had mild learning difficulties, hearing loss, and visual impairment. He was sensitive to the sun from birth and had dry, atrophic skin and irregular pigmentation on sun-exposed areas. Laboratory studies indicated renal insufficiency, and he died at the age of 16 years from severe pneumonia and multisystem organ failure. This individual had many features in common with XPCS1CD, but there was no report of pancytopenia. He was homozygous for p.Arg153Pro in XPF.

(C) The heterozygous c.706T>C SNV in *ERCC4* exon 4 and the heterozygous c.1765C>T SNV in XPCS1CD. The altered amino acids, Cys236 and Arg589, are shown in red.
(D) The structure of ERCC1 and XPF and the amino acid alterations reported here and published previously.[18–20] The cases shown in colors are as follows: XP, black; COFS, blue; XFE, green; and CS or XPCS, red. Superscripted 1 and 2 designate the number of discrete alleles.

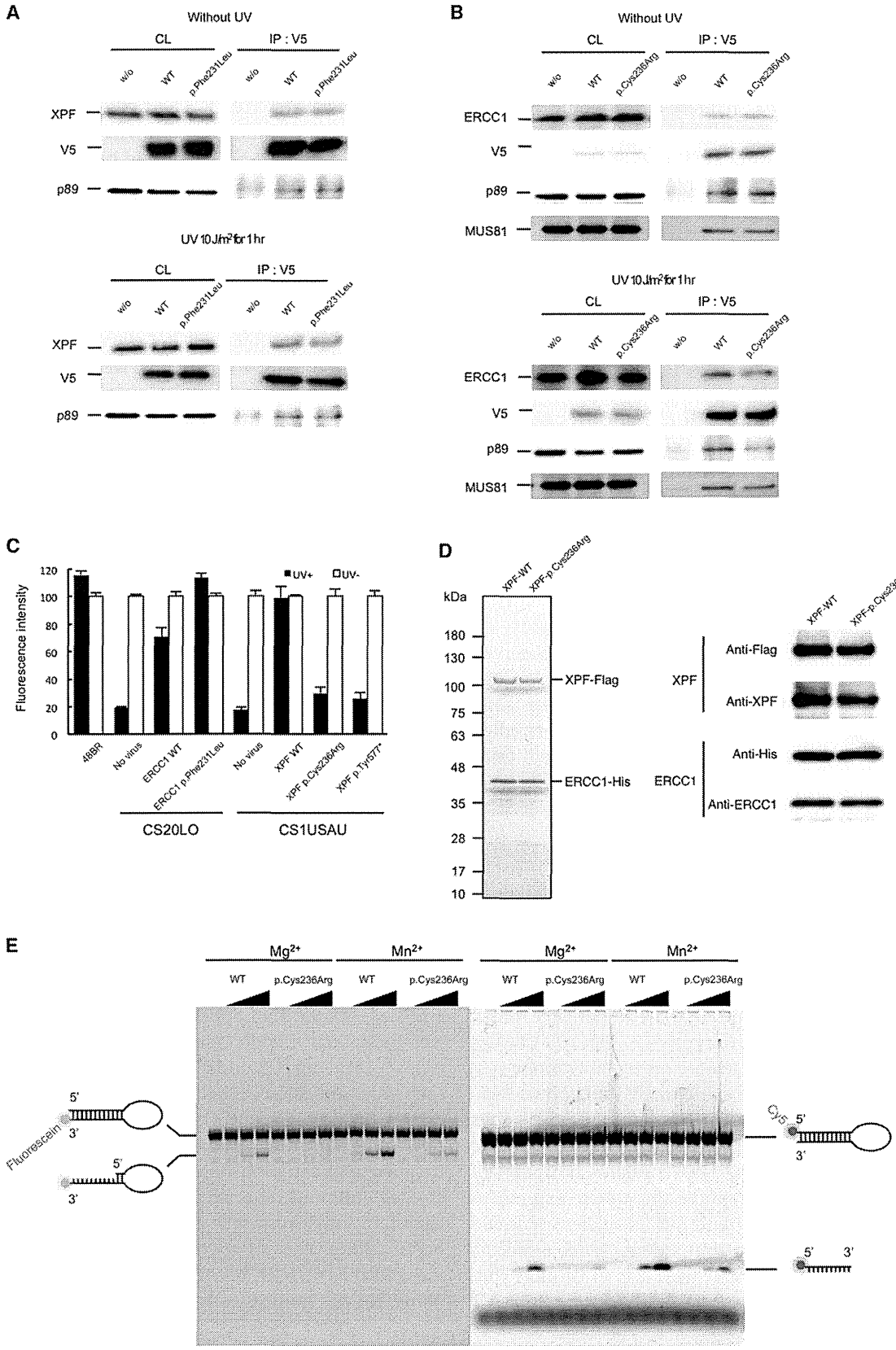


**Figure 3. ERCC1 and XPF Interaction in the CS Cells**

(A) V5-tagged wild-type and p.Phe231Leu altered ERCC1 interactions with the endogenous wild-type XPF were assayed by immunoprecipitation either without UV irradiation or 1 hr after 10 J/m$^2$ of UV irradiation.

(B) V5-tagged wild-type and p.Cys236Arg altered XPF were expressed in 293T cells, and interactions with the endogenous wild-type ERCC1 were assayed by immunoprecipitation from extracts of cells either without UV irradiation or 1 hr after 10 J/m$^2$ of UV irradiation.

*(legend continued on next page)*

**Table 1. Primers Used for Allele-Specific Amplifications**

| Primer Designation | Primer Sequence |
|---|---|
| ERCC1-WT1 | 5′- CTGATGGAGAAGCTAGAGCAGGACTTC-3′ |
| ERCC1-p.Phe231Leu | 5′- CTGATGGAGAAGCTAGAGCAGGACTTG-3′ |
| ERCC1-com1 | 5′- CCTGATGGAGAAGCTAGAGCAGGACTT-3′ |
| ERCC1-Rv1 | 5′- GGTCAGACATTCAGTCACCCGC-3′ |
| XPF-WT1 | 5′- GACTGCTATACTGGACATTTTAAATGCAT-3′ |
| XPF-p.Cys236Arg | 5′- GACTGCTATACTGGACATTTTAAATGCAC-3′ |
| XPF-com1 | 5′- AGACTGCTATACTGGACATTTTAAATGCA-3′ |
| XPF-Rv1 | 5′- TCCAAGCTGGTGCCACAAA-3′ |
| XPF-WT2 | 5′- AGGGTACTACATGAAGTGGAGCCAAGAT AC-3′ |
| XPF-p.Tyr577* | 5′- AGGGTACTACATGAAGTGGAGCCAAGAT AA-3′ |
| XPF-com2 | 5′- AAGGGTACTACATGAAGTGGAGCCAAGA TA-3′ |
| XPF-Rv2 | 5′- CCCTCAGAGGTTTCCCAGGC-3′ |

Somewhat surprisingly, the previously reported *ERCC1*-deficient severe COFS individual was compound heterozygous for the same pathogenic p.Phe231Leu change together with a termination substitution, p.Gln158*,[21] whereas our CS type II individual was homozygous for this substitution. Because the p.Phe231Leu altered ERCC1 retained normal function, differences in severity of the clinical features might be explained by the dosage of *ERCC1* expression. We hypothesize that the relatively milder clinical features observed in our CS individual might be due to the fact that the biallelic expression of the mutated *ERCC1* allele produced twice the level of functional ERCC1 in the CS individual as in the COFS individual. This idea is also supported by the observation that the other *ERCC1*-deficient XP individual, who displayed milder clinical features, harbored a splice-site mutation that most likely allowed readthrough of a significant amount of normal protein.

We identified a heterozygous XPF alteration, p.Cys236Arg, in CS individuals CS1USAU and XPCS1CD. CS1USAU displayed mild skin problems in the range defined by normal CS features, but he has been very well protected from sun exposure. He displayed hypopigmented macules (Figure 1A), which are typical of XP and often occur on the limbs and other sun-exposed sites before "freckling." In view of this and his early freckling, it seems appropriate to classify this affected individual as also having the combined XPCS phenotype. However, XPCS1CD, but not CS1USAU, also exhibited hematological abnormalities characteristic of FA. Surprisingly, the second allele in the milder individual, CS1USAU, was a functionally null termination mutation, which was subjected to NMD, whereas in the more severely affected XPCS1CD, the second allele harbored c.1765C>T (p.Arg589Trp), which is found in several XP individuals and results in mislocalization of the ERCC1-XPF complex to the cytoplasm and thus causes a severe XP phenotype when combined with certain other alleles.[19] XP32BR (with p.Arg589Trp and p.Pro379Ser) was a mildly affected XP individual in his teens and had no neurological problems; XP24BR (with p.Arg589Trp and p.Arg799Trp) was also mildly affected but is now showing some abnormal neurological and CS-like facial features in her 40s (our unpublished data); AS871 (with p.Arg589Trp resulting from

Interactions were detected by immunoblotting with antibodies against the V5-tagged ERCC1 and XPF (1H6, MBL), MUS81 (MTA30 2G10/3, Santa Cruz), ERCC1 (8F1, Santa Cruz), and XPF (Ab-1, Thermo scientific). Abbreviations are as follows: CL, crude lysate (10% load); and IP, immunoprecipitate.

(C) Rescue of the RRS deficiency was assayed by the infection of recombinant lentivirus expressing either wild-type or mutant *ERCC1* and *ERCC4* cDNAs (filled bars, 11 J/m$^2$ UV; empty bars, no UV). RRS was normalized to activity in nonirradiated cells. Error bars represent the SD of medians of nuclear fluorescence measurements in quintuplicate samples.

(D) Purification of the recombinant ERCC1-XPF complexes. FLAG-tagged (C terminus) wild-type and p.Cys236Arg altered XPF were coexpressed with the 6 × His-tagged ERCC1 (C terminus) in 293T cells. The cells were harvested and lysed in lysis buffer (50 mM Tris-HCl, 150 mM KCl, 1 mM EDTA, 1% NP-40, 10% glycerol, 0.25 mM PMSF, protease-inhibitor cocktail [PIC, Roche], pH 7.5). Tandem affinity purification was performed with mouse anti-FLAG IgG-conjugated beads (M2 agarose, SIGMA) followed by TALON metal affinity resin (Clontech). Cell lysates were incubated with anti-FLAG agarose beads and were subsequently washing with salt buffer (20 mM Tris-HCl, 1 M KCl, 0.1 mM EDTA, 10% glycerol, PIC, pH 7.5) and starting buffer (20 mM Tris-HCl, 800 mM KCl, 10% glycerol, 10 mM imidazole, PIC, pH 7.5). Binding proteins were eluted with starting buffer containing 1 mg/ml FLAG peptide. The eluted fractions were incubated with TALON metal affinity resin (Clontech) and were then sequentially washed with buffer A (40 mM HEPES, 1,000 mM NaCl, 10% glycerol, 10 mM Imidazole, PIC, pH 7.5) and buffer B (40 mM HEPES, 100 mM NaCl, 10% glycerol, 10 mM Imidazole, PIC, pH 7.5). The purified complex was sequentially eluted with elution buffer A (40 mM HEPES, 100 mM NaCl, 10% glycerol, 100 mM Imidazole, PIC, pH 7.5) and elution buffer B (40 mM HEPES, 100 mM NaCl, 10% glycerol, 300 mM Imidazole, pH 7.5). Purified complex was dialyzed against GF buffer (25 mM HEPES, 150 mM NaCl, 10% glycerol, 5 mM beta-mercaptoethanol, PIC, pH 8.0) and concentrated. The purified complexes were resolved by SDS-PAGE and detected by silver staining (100 ng of total protein). Purity of the complexes was assessed by immunoblotting with antibodies against the FLAG (MBL) and 6 × His (MBL) tags, as well as ERCC1 and XPF. No endogenous XPF was detected.

(E) Endonuclease activity of the wild-type and altered ERCC1-XPF complexes was determined with fluorescently labeled 12 bp stem-dT22-loop DNA templates. Either 3′-fluorescein- or 5′-Cy5-labeled oligonucleotides (5′-GCCAGCGCTCGG-dT22-CCGAGCGCTGGC-3′) were purchased from SIGMA and self-annealed in TE buffer. Nuclease incision reactions were performed on 200 fmol of the DNA templates and 0, 25, 50, 100 ng of the purified ERCC1-XPF complexes in a total volume of 15 μl nuclease reaction buffer (25 mM HEPES, 40 mM NaCl, 10% glycerol, 0.5 mM beta-mercaptoethanol, and 0.1 mg/ml BSA and either 2 mM $MgCl_2$ or 0.4 mM $MnSO_4$, pH 8.0). The reaction mixtures were incubated at 30°C for 1 hr. Samples were separated on urea-denatured 15% PAGE, and the cleaved products were analyzed by a Typhoon imager (GE).

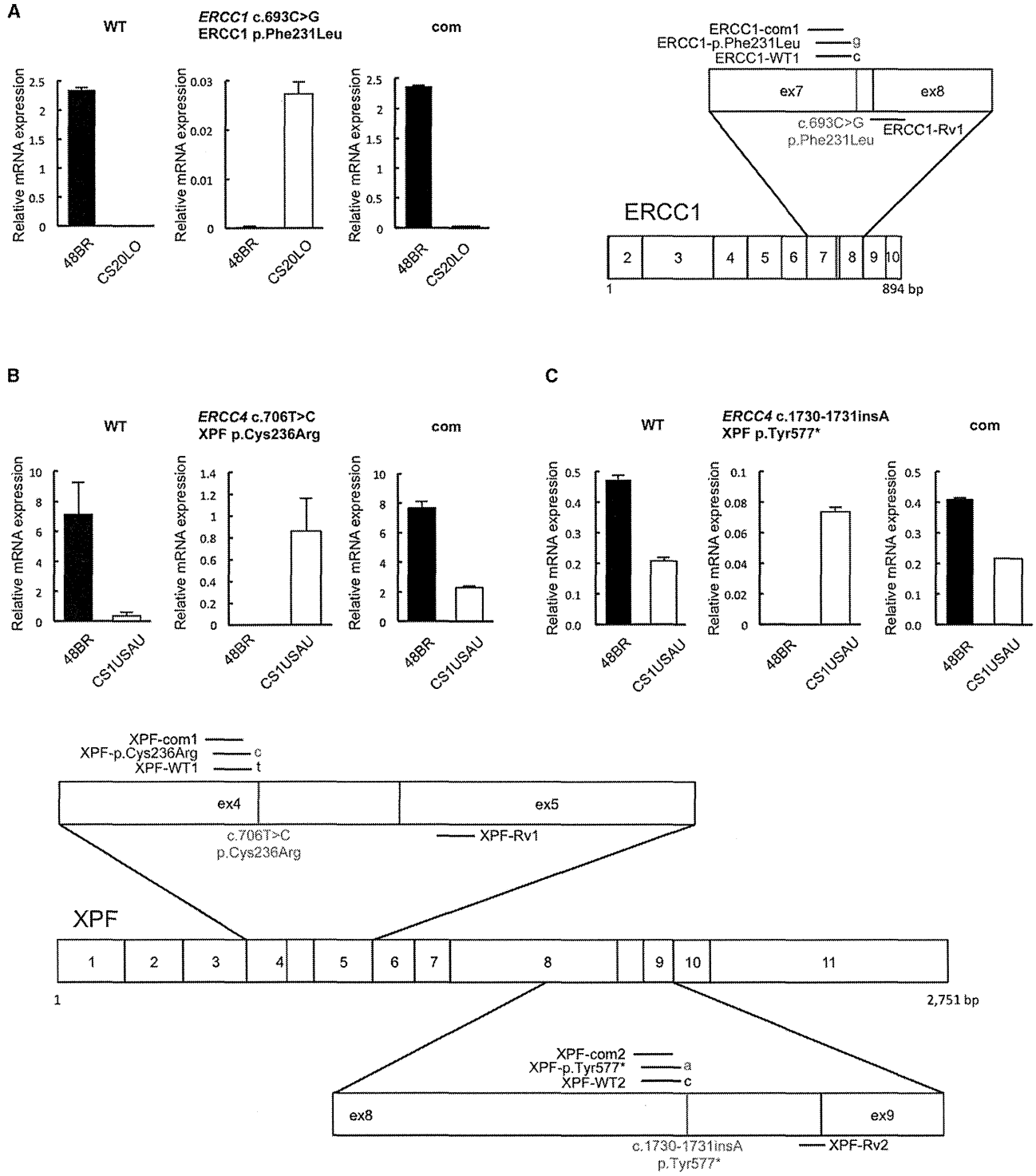


**Figure 4. Expression of the Pathogenic Alleles in the CS Cells**

Total RNA was extracted with ISOGEN reagent (NIPPON GENE) according to the manufacturer's instruction. One microgram of total RNA was reverse transcribed with a high-capacity RNA-to-cDNA kit (Applied Biosystems, Life Technologies). Quantitative PCR amplification and real-time detection were carried out in a Thermal Cycler Dice Real-Time System (TaKaRa Bio) with SYBR Premix Ex TaqII (TaKaRa Bio) and a QuantiTect SYBR Green PCR kit (QIAGEN). For each sample, relative mRNA levels were normalized against *HPRT1* mRNA expression. Error bars represent the SD of means of triplicate experiments.

(A) Selective quantitative amplification of the wild-type and the mutated c.693C>G (p.Phe231Leu) *ERCC1* alleles in CS20LO cells and normal 48BR cells. Allele-specific primers selectively amplified the wild-type (c.693C) allele (ERCC1-WT1 and ERCC1-Rv1, left panel), the CS pathogenic mutant (c.693C>G) allele (ERCC1-p.Phe231Leu and ERCC1-Rv1, middle panel), and both alleles at once (ERCC1-com1 and ERCC1-Rv1, right panel).

(B) Selective quantitative amplification of the wild-type and the mutated c.706T>C (p.Cys236Arg) *ERCC4* alleles in CS1USAU cells and normal 48BR cells. Allele-specific primers selectively amplified the wild-type (c.706T) allele (XPF-WT1 and XPF-Rv1, left panel), the CS

*(legend continued on next page)*